RYAN

N69-30745

(ACCESSION NUMBER)	(THRU)
75	1
(PAGES)	(CODE)
NASA CR-101775	13
(NASA CR OR TMX OR AD NUMBER)	(CATEGORY)

NASA CR 101??5

SCATTEROMETER DATA ANALYSIS
PROGRAM
FINAL REPORT

REPORT NO. 57667-3

For the Period 18 October 1967 to 31 May 1968

PREPARED FOR

NASA MANNED SPACECRAFT CENTER
HOUSTON, TEXAS
UNDER CONTRACT NO. NAS 9-6059

RYAN AERONAUTICAL COMPANY
5650 KEARNY MESA ROAD
SAN DIEGO, CALIFORNIA 92112

TABLE OF CONTENTS

LIST OF ILLUSTRATIONS

LIST OF ILLUSTRATIONS

LIST OF TABLES

SECTION 1

INTRODUCTION

The outstanding results obtained from REDOP scatterometer data during this contract period are proof of the scatterometer's ability to identify sea state (ocean surface roughness) quantitatively and to identify several ice types, which are associated with ice thickness. Further development of detection capabilities in these two areas will establish scatterometers as earth resources instruments of great value.

Two sea-state missions were flown during this contract period, one to Newfoundland and one to Iceland. The purpose of both missions was to collect data from high seas. The mission to Newfoundland resulted in data from 13-foot seas. The mission to Iceland resulted in data from 9-, 19- 26-foot seas. The results of these and other missions are discussed in Section 2 of this report.

Other significant accomplishments include the development of a low-cost fully-automated data processing system and new display techniques. Fully-automated data processing has been developed through close coordination between Ryan and the Computation and Analysis Division of MSC. The fully-automated data reduction techniques have resulted in a ten-to-one decrease in data processing costs. A new technique of displaying scatterometer data was developed. This technique is known as the Spatially Adjusted Time History (SATH) plot. This type of data presentation will greatly assist the Principal Investigators in data analysis.

Model theory can be used to assist in data analysis by the correlation of terrain features with signal characteristics. A discussion of model theory is presented in Section 5 of this report.

An important task has been preparations for reduction of 400 MHz scatterometer data. These preparations have included a study of its characteristics and capabilities, a preliminary error analysis, and a digital computer program for reducing data. The study and analysis tasks concerning the 400 MHz scatterometer are presented in Section 6.

The original objectives of the Scatterometer Data Analysis Project for the Earth Resources Survey was to study, reduce, analyze and correlate data for MSC. Data from several sources were collected and processed according to the defined objectives. The success realized from this program is described in the following text.

SECTION 2

DATA REDUCED AND EVALUATED

This section lists all the lines and runs which have been reduced, evaluated and released through the Test and Operations Office to Earth Resources Principal Investigators (Table 2-1). Also included are descriptions of each mission and samples of data.

2.1 MISSION 32, FLIGHT 1

Mission 32, Flight 1 was over the Lawrence and Garden City, Kansas test sites for the University of Kansas and the United State Geological Survey. These sites are both farmland areas with different types of crops and cultivated fields. Studies are being conducted to correlate various crop configurations with characteristic changes in reflectivity. Further plans are being made to examine these type sites at various times of the year to determine changes in reflectivity with the seasonal variations in crop size and distribution. An example of data from this mission is shown in Figure 2-1.

2.2 MISSION 34, FLIGHT 2

Figure 2-2 is data gathered on Mission 34. Flight 2 was designed for ESSA and the Naval Oceanographic Office, to collect reflectivity data from an area designated as the Gulf Stream North, located at 36° 17'N and 73° 41'W. The waves measured over the Gulf Stream were somewhere between 4.8 and 5.4 feet which corresponds to a wind from 9 to 16 knots. This is a sea-state bordering between 3 and 4 (Ref. 1) or a moderate sea. Many experiments have been carried out in this area for the purpose of studying and mapping the boundaries of the Gulf Stream current. The possibilities of mapping through detection of temperature variations is good. However, variations in sea state conditions may occur between the current and the

Table 2.1 List of Evaluated Lines and Runs

MISSION	FLIGHT	LINE	RUN	
32	1	2	1	(aft only)
32	1	4	1	(fore only)
34	2	1	3	
34	2	1	4	
34	2	1	5	
34	2	2	2	
34	2	2	3	
34	2	2	4	
38	4	91	1	
38	4	93	3	
38	4	93	4	
44	1	1	1	
44	1	1	2	
47	3	91	1	
47	5	92	2	
47	6	94	1	
60	1	91	1	
60	1	92	1	
60	1	92	2	
60	1	91	2	
60	2	93	1	
60	2	94	1	
60	2	94	2	
60	2	93	2	
70	2	1	1	
70	2	2	1	
70	2	3	1	
70	2	4	1	
70	3	10	1	
70	3	11	1	
70	3	12	1	
70	3	13	1	
70	4	21	1	
70	4	22	1	
70	4	23	1	
70	4	24	1	

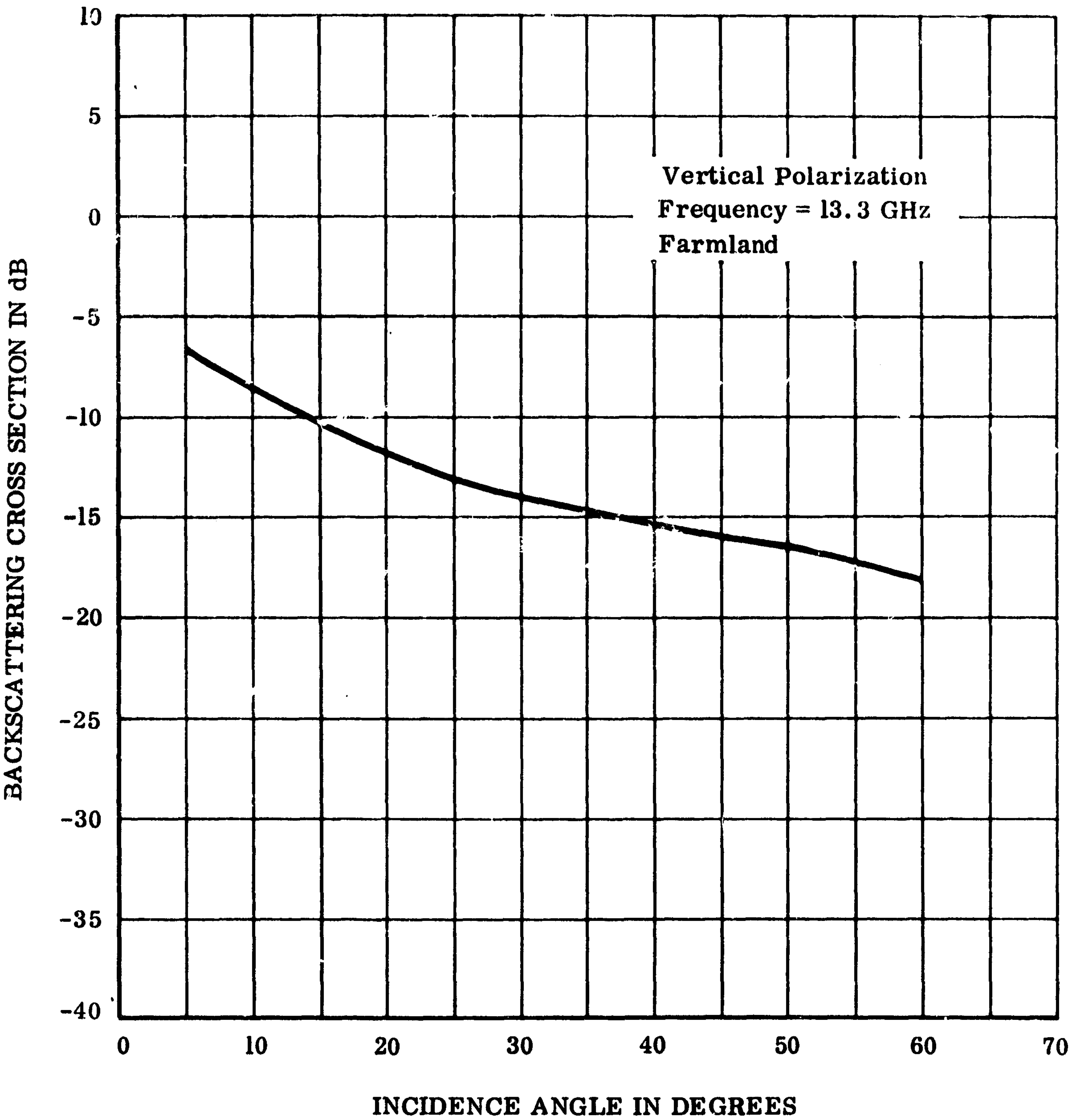

Figure 2-1 Scatterometer Reflectivity of Typical Farmland Garden, City, Kansas Mission 32, Flight 1, Line 2

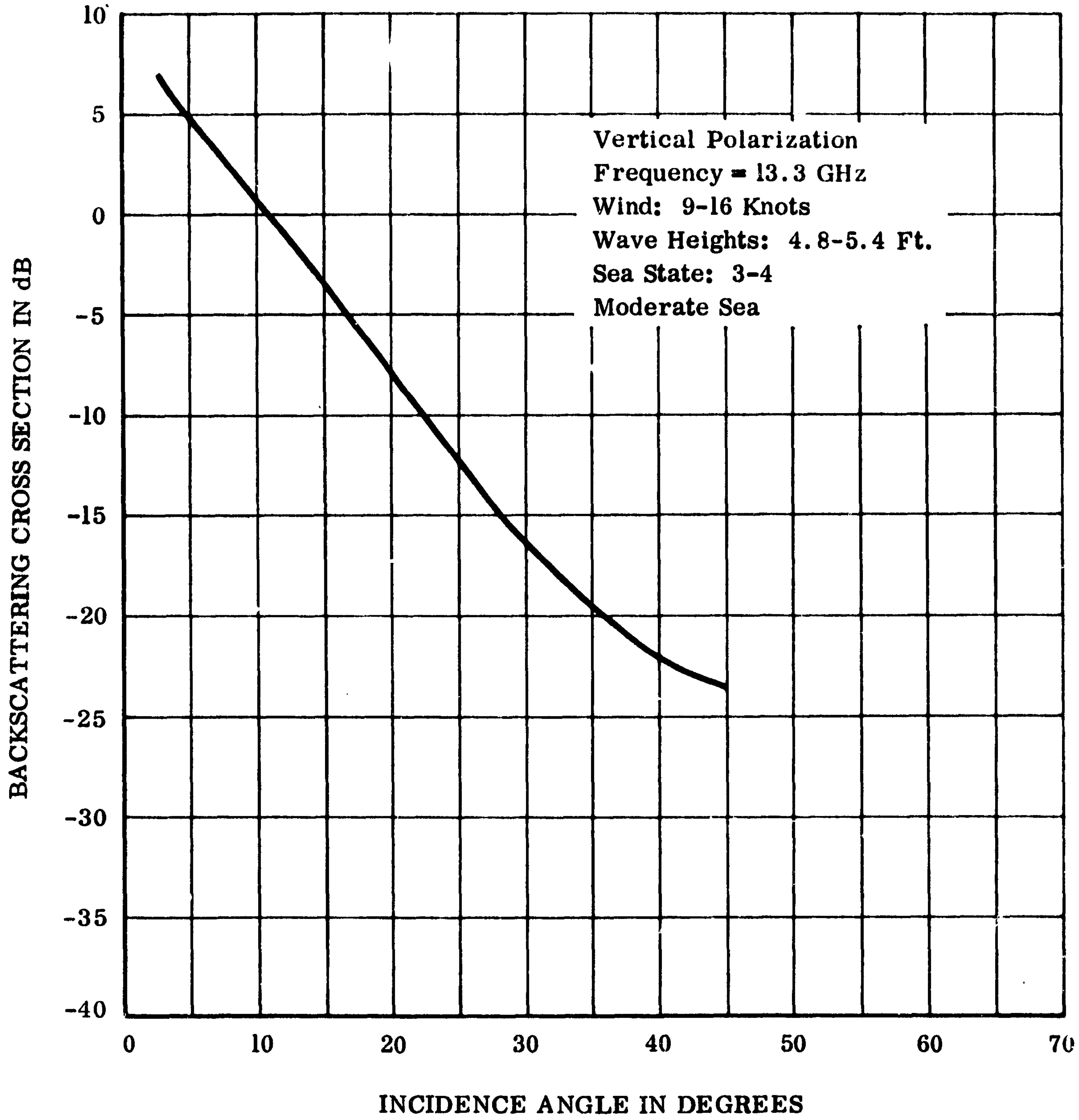

Figure 2-2 Scatterometer Reflectivity of Gulf Stream
Gulf Stream North Mission 34, Flight 2, Line 2

surrounding sea.. If these differences exist due to differential water movement, then a change in scatterometer signals should also occur. The final results of this experiment are not yet available and time/history curves have not been examined in detail.

2.3 MISSION 38, FLIGHT 4

Mission 38 had the primary objective of gathering radar scatterometer data over high sea conditions in support of the U.S. Naval Oceanographic Office (NOO); however, only light sea conditions prevailed during the entire mission.

The site selected was the area around Bermuda Island which included flights over Bermuda and Argus Island southwest of Bermuda. Figure 2-3 shows an averaged curve from Mission 38. Observations made by the pilot and the crew indicated winds around 1 knot and wave heights less than 1 foot.

2.4 MISSION 44, FLIGHT 1

Mission 44, flight 1 was in support of studies being conducted by the University of Nevada. The Arizona Sedimentary test site, where the data (Figure 2-4) was gathered, has coordinates 36° 42' N to 36° 33' N and 113° 47' W. This test area has been covered quite extensively by ground truth teams from the University of Nevada. All terrain variations have been identified catagorized and mapped. Data, in the form of $\sigma_o(\theta)$ curves has been reduced and released for detailed analysis. In addition, a new real-time data analysis technique is being applied which gives discrete information. It has been named the Spatially Adjusted Time History (SATH) technique (Section 4).

2.5 MISSION 47, FLIGHTS 3, 5 AND 6

Mission 47, flights 3, 5 and 6 were flown from Point Barrow, Alaska. The analyzed data (Figure 2-5) was gathered over ice in support of studies being conducted by the University of Kansas. Using aerial photography,

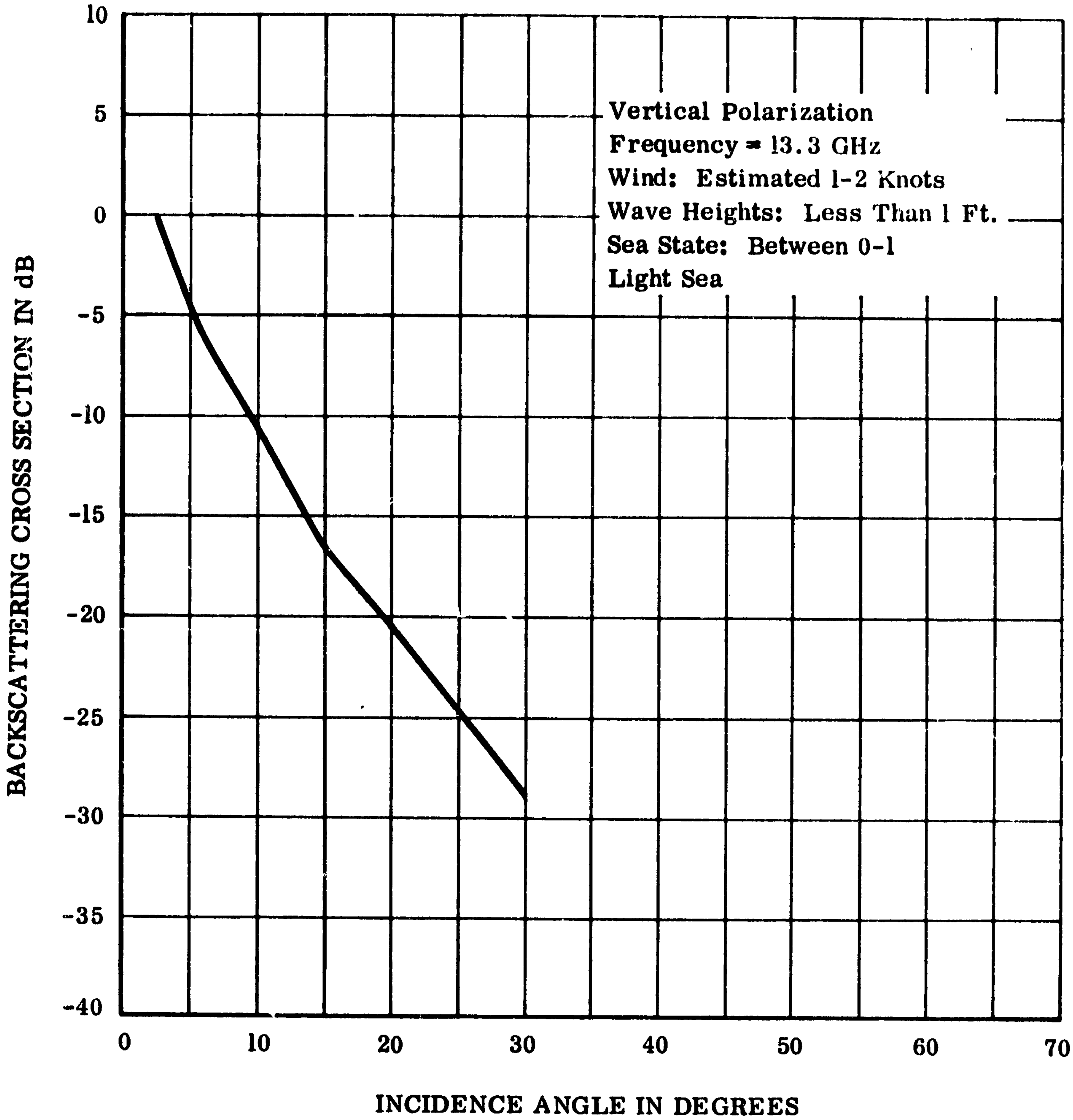

Figure 2-3 Average Scatterometer Reflectivity of Ocean, Bermuda Area
Mission 38, Flight 4, Lines 91 and 93

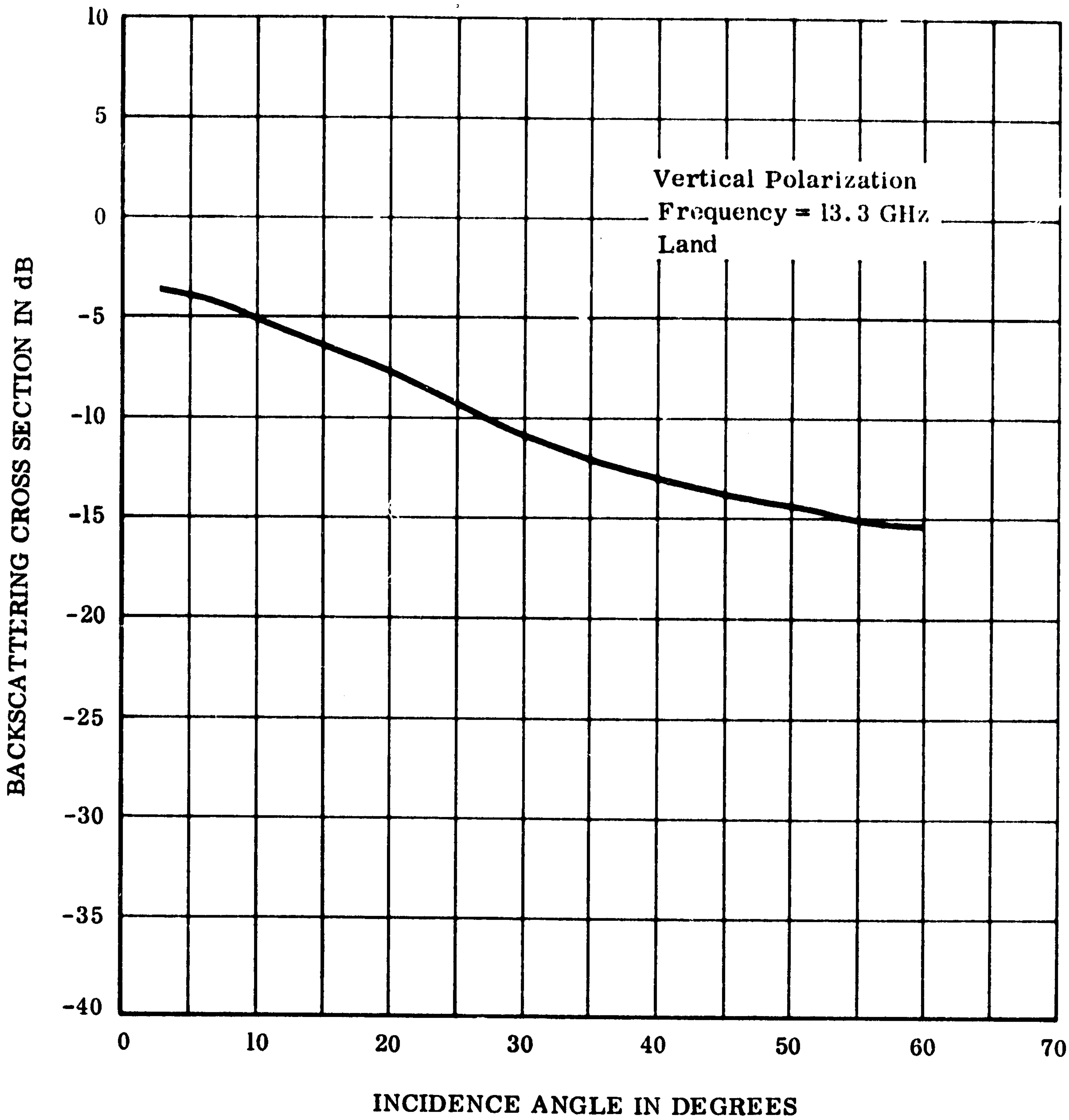

Figure 2-4 Scatterometer Reflectivity Sediments, Arizona Sedimentary Site, Mission 44, Flight 1, Line 1

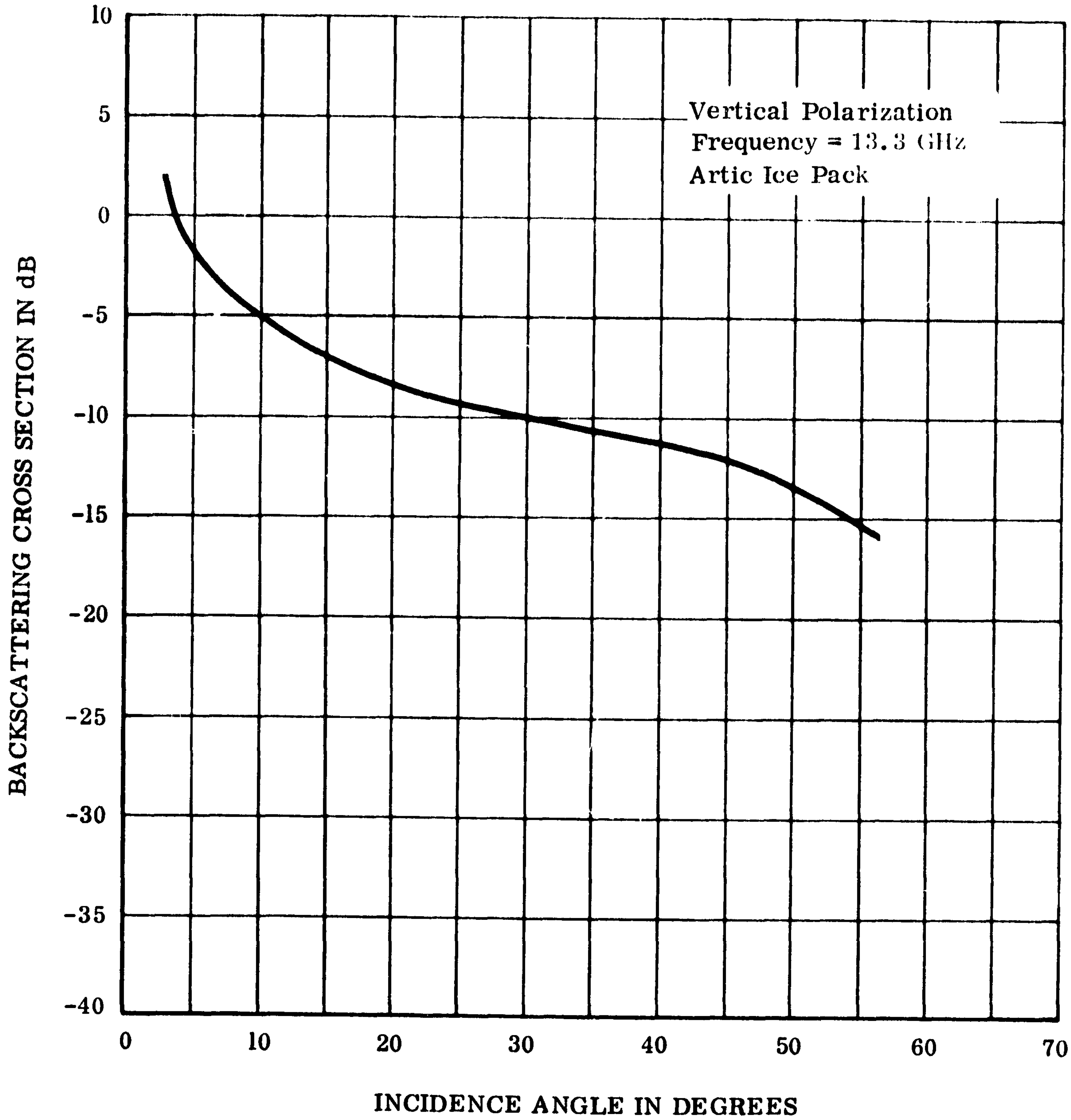

Figure 2-5 Scatterometer Reflectivity of Arctic Ice Pack, Point Barrow Alaska, Mission 47, Flight 5, Line 92

ground truth data, and scatterometer output in oscillograph trace format, correlations were made between several changes in ice and characteristic changes in signal level. By choosing a 2.5 degree incidence angle it was possible to note transitions between several different types of ice, for example winter ice and polar ice. Also, areas with variable ice types were detected by changes in the signal level, such as smooth and rough winter ice. Pressure ridges in ice flows were easily detected and correlated with the expected signal changes as reported by Rouse[2]. Detailed studies are being conducted to determine the extent to which REDOP scatterometers can be used to differentiate subtle changes in ice conditions.

2.6 MISSION 60, FLIGHTS 1 AND 2

Mission 60 was an oceanographic mission based in Newfoundland, Canada. This mission was designed to obtain scatterometry data for high sea states. The mission was seeking either of two possible environmental conditions. The first, and more desirable, was a wind of at least 25 knots blowing from land toward the open sea. This condition would produce a fully developed sea with wave heights that increase with distance from the shoreline. The second was a wind of at least 25 knots blowing parallel to the shoreline. The actual wind conditions during Mission 60 were of the second type with velocities of from 28 to 30 knots. Significant wave heights were around 13 feet.

Figure 2-6 is a family of backscattering curves from Mission 60 relating the direction of wind and wave movement to REDOP scatterometer data. The upwind curve was taken from the aft data* from cells 3 and 4, maps A, B, C, and D (Figure 2-7 a, b, c, d, respectively) and the fore data from cells 7 to 13 and 23. The downwind curve was averaged from the fore data

---

*Aft data is the doppler component received from the aft part of the fan beam antenna, 0 to -60°, where the fan beam is taken in the airplane fore-aft, or longitudinal, direction. The fore data is the doppler component received from the forward part of the antenna beam, 0 to 60°.

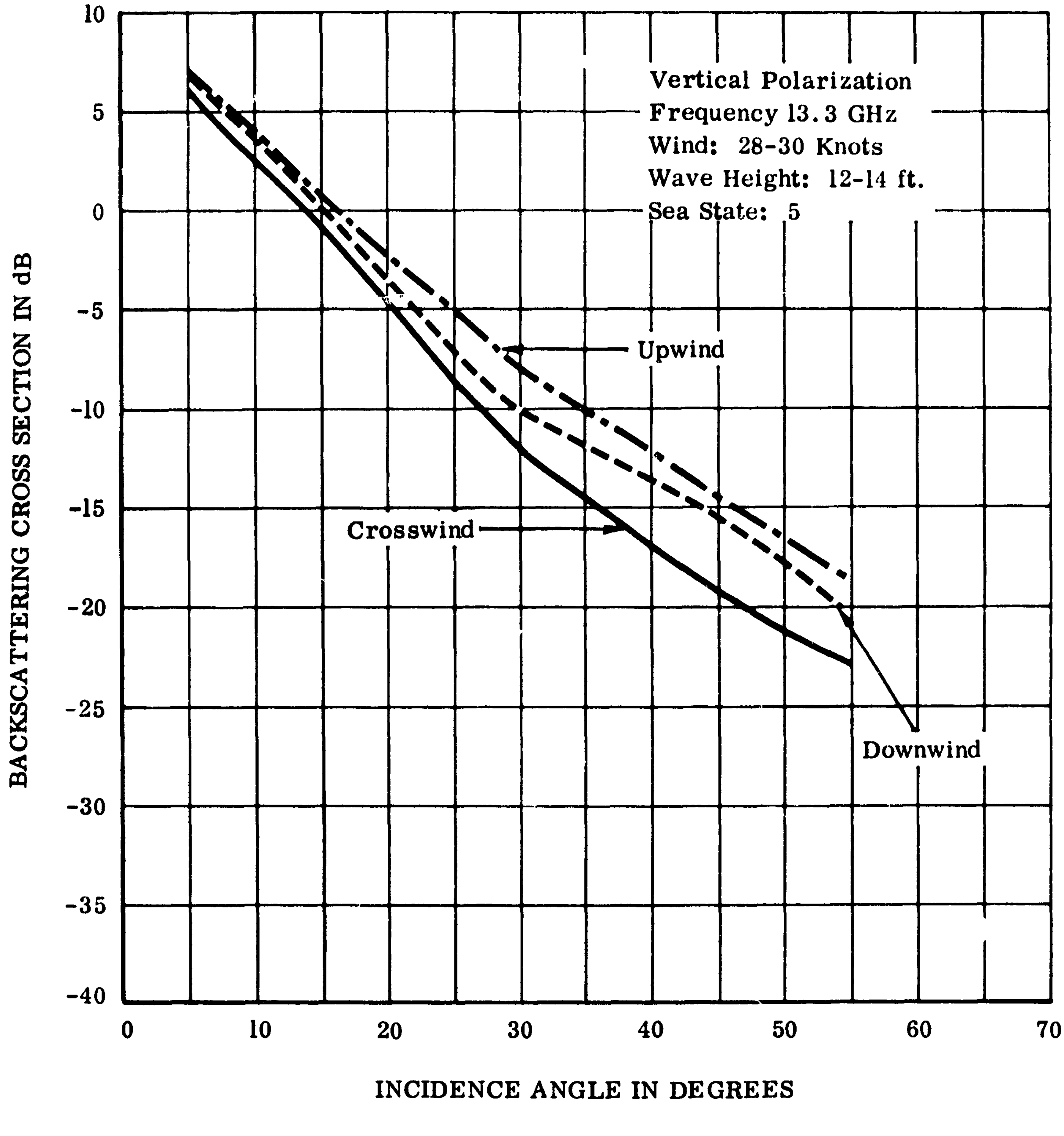

Figure 2-6 Scatterometer Reflectivity of Atlantic Ocean Newfoundland, Canada, Mission 60, Lines 1 and 2

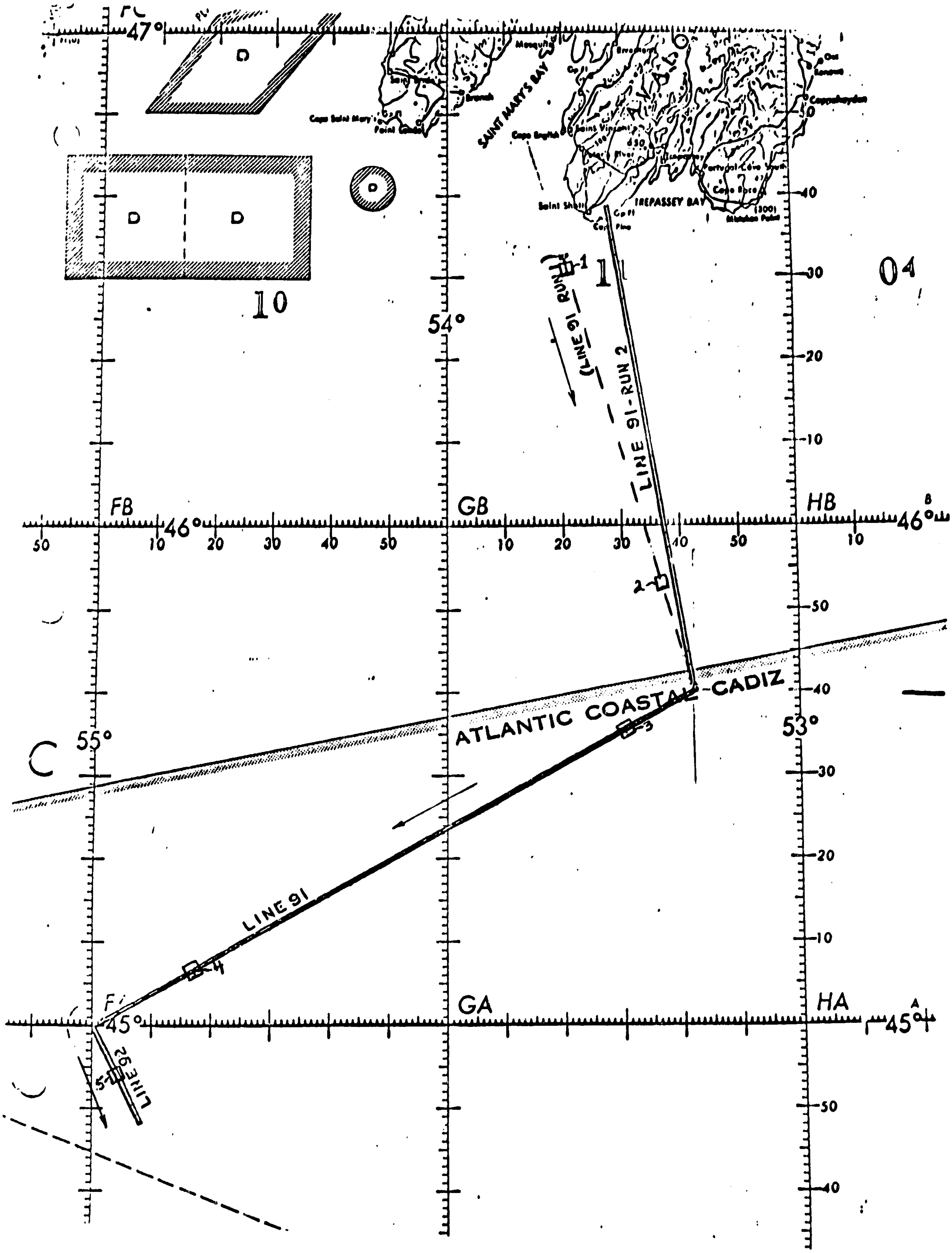

Figure 2-7a Map A - Flight Lines 91 and 92, Run 1 Newfoundland, Canada

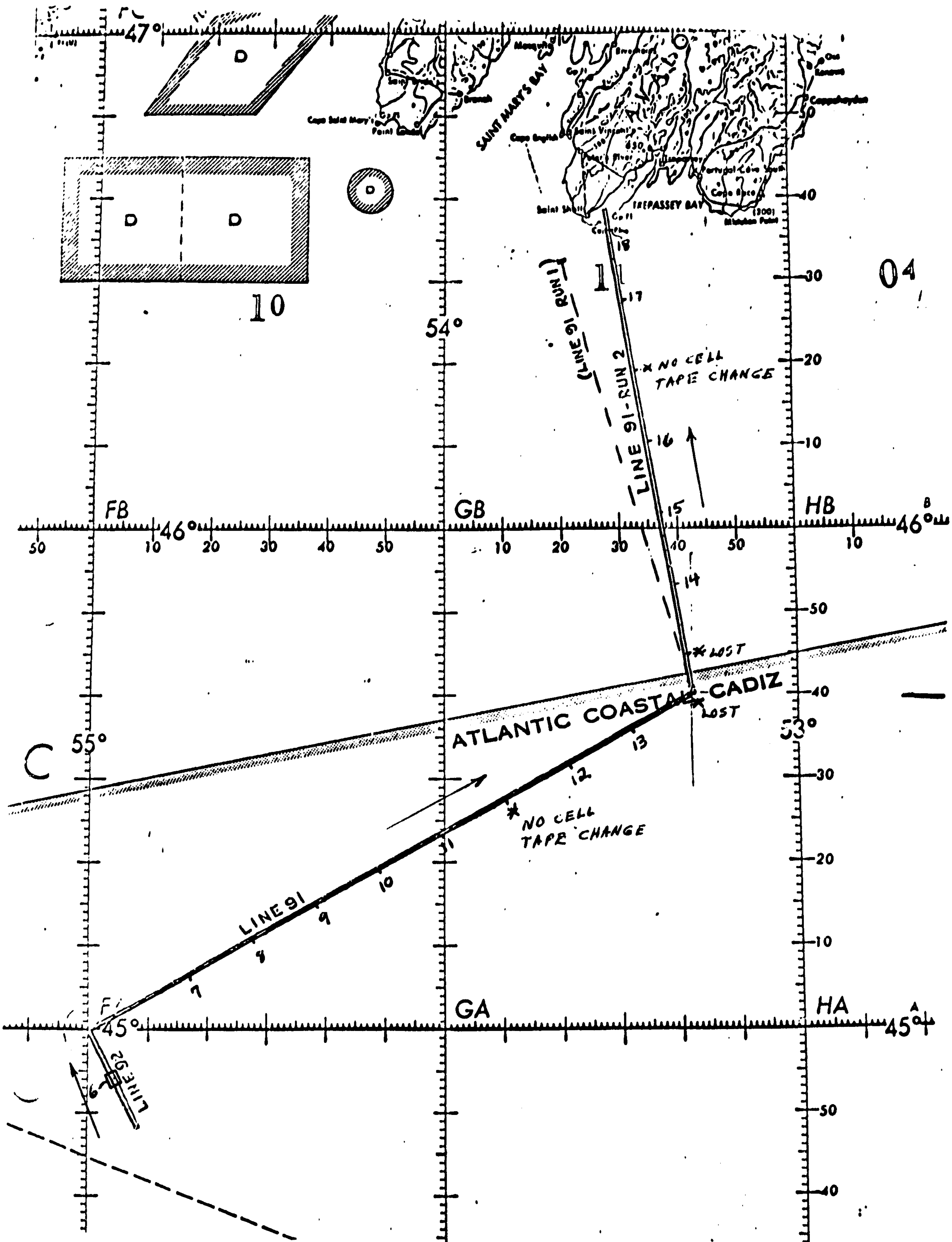

Figure 2-7b Map B - Flight Lines 91 and 92, Run 2, Newfoundland, Canada

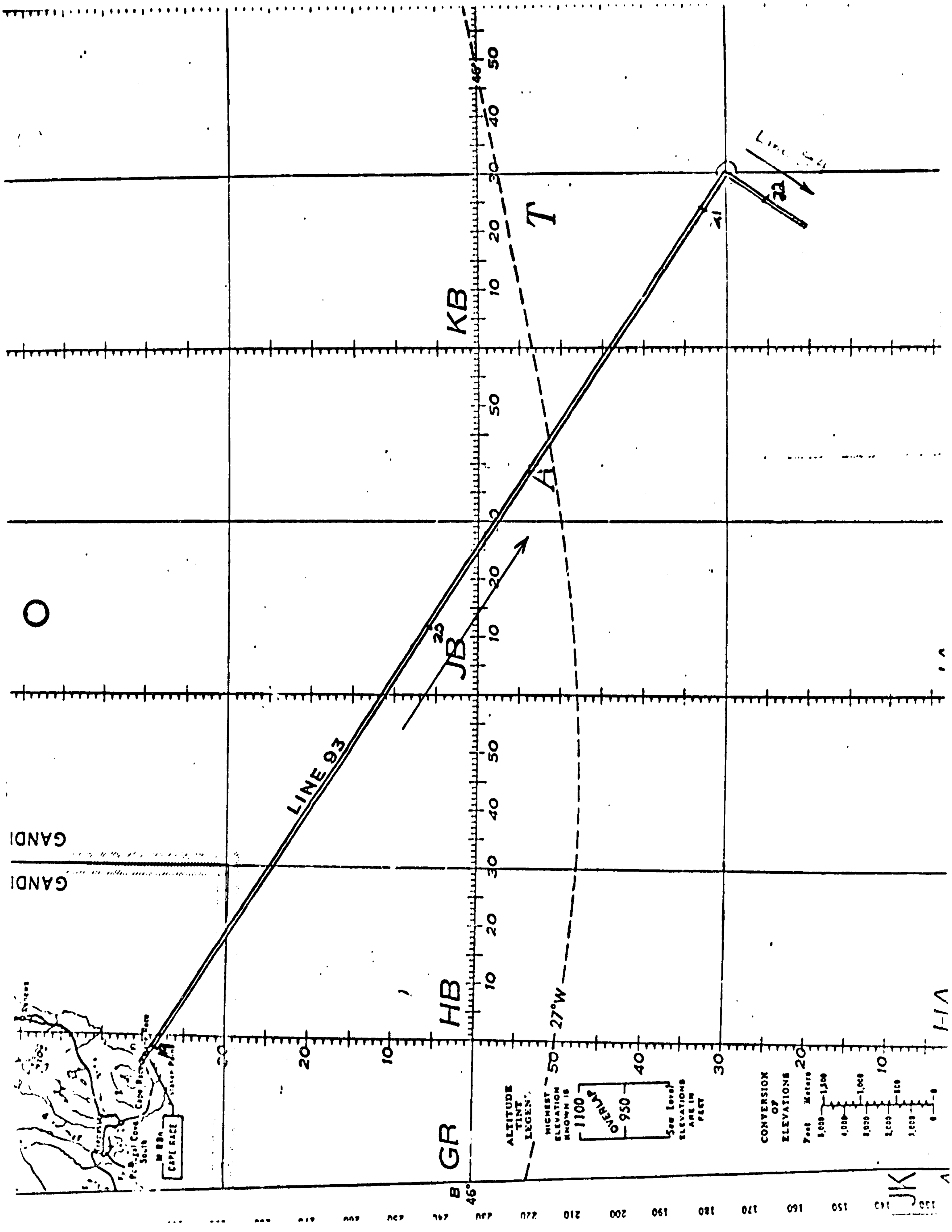

Figure 2-7c Map C - Flight Lines 93 and 94, Run 1 Newfoundland, Canada

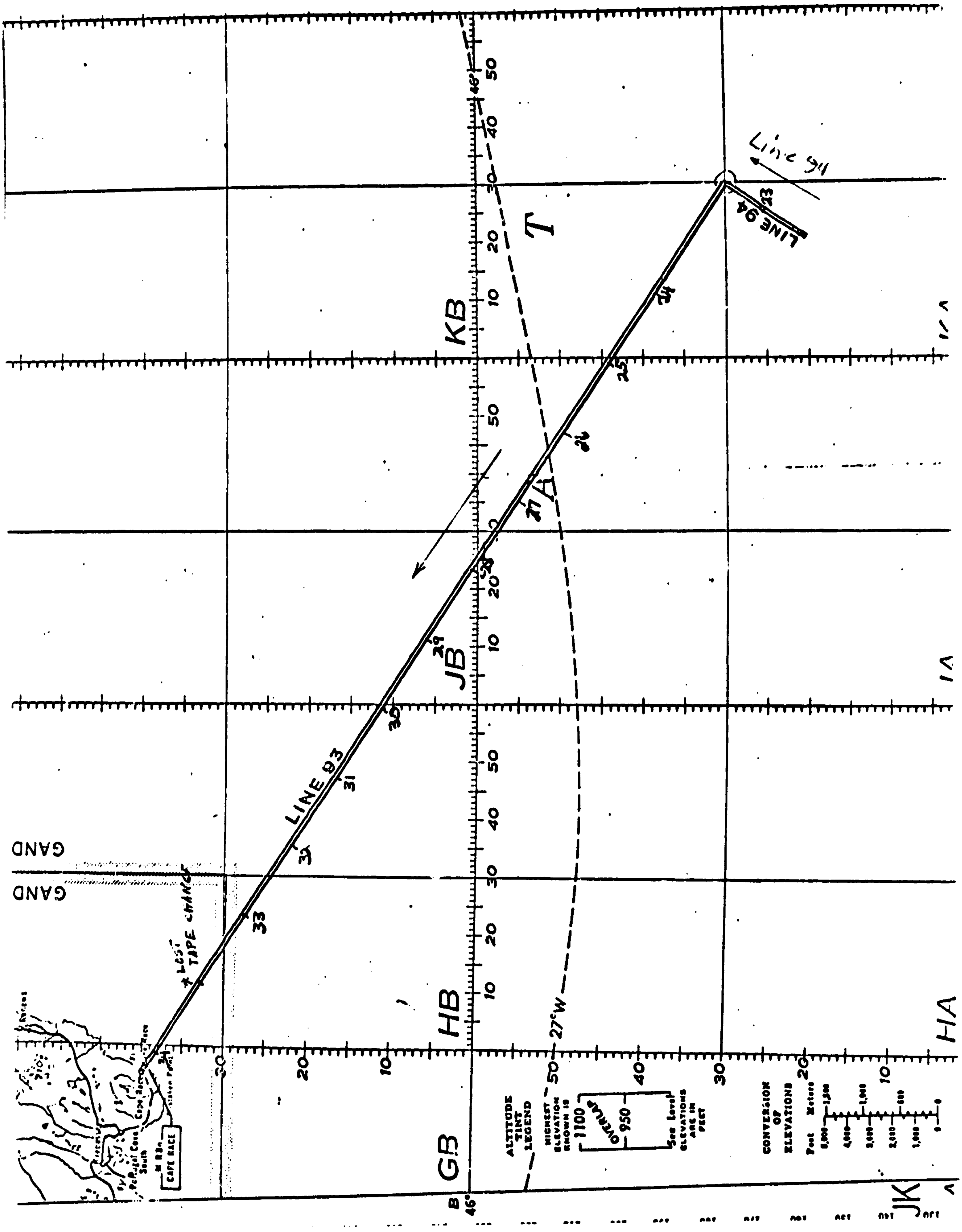

Figure 2-7d Map D - Flight Lines 93 and 94, Run 2, Newfoundland, Canada

of cells 3 and 4, the aft data of cells 7 through 13, and the aft data of cell 23. The crosswind curve is an average of fore and aft data from resolution cells 1, 2 and 5, cells 14 through 18 and cells 24 through 29. These groupings were made after studying Figure 2-8 (which shows wind conditions during the flight) and correlating times when wind conditions were similar.

From this data it can be concluded that sea surface conditions are detectable with a 13.3 GHz scatterometer. Also wind direction producing sea conditions may be determined from reduced data.

2.7 MISSION 70, FLIGHTS 2, 3 AND 4

Keflavik, Iceland was the base of operations for Mission 70. The objective of this mission was to gather data from rough sea surface conditions. The predicted weather circumstances did arise and data was collected from an approximate sea state 7 (26 foot waves) condition. Data was also obtained from lesser sea states of 5 and 6.

The information gathered has been reduced by hand to obtain quick-look preliminary results. Further analyses and computer processing are to be carried out in the immediate future.

Figure 2-9 is a representative curve from each sea state encountered on this mission together with data for lower sea-states from missions 34 and 38. The data is consistent, i.e., the roughest sea state yields the highest return at the higher angles and the lowest return at the lower angles. It is noted, however, that the wave heights indicated are preliminary visual estimates only. Definitive assignment of data to specific sea-state and wind conditions will be done by the Principal Investigator after correlation of data with the meteorological hindcast.

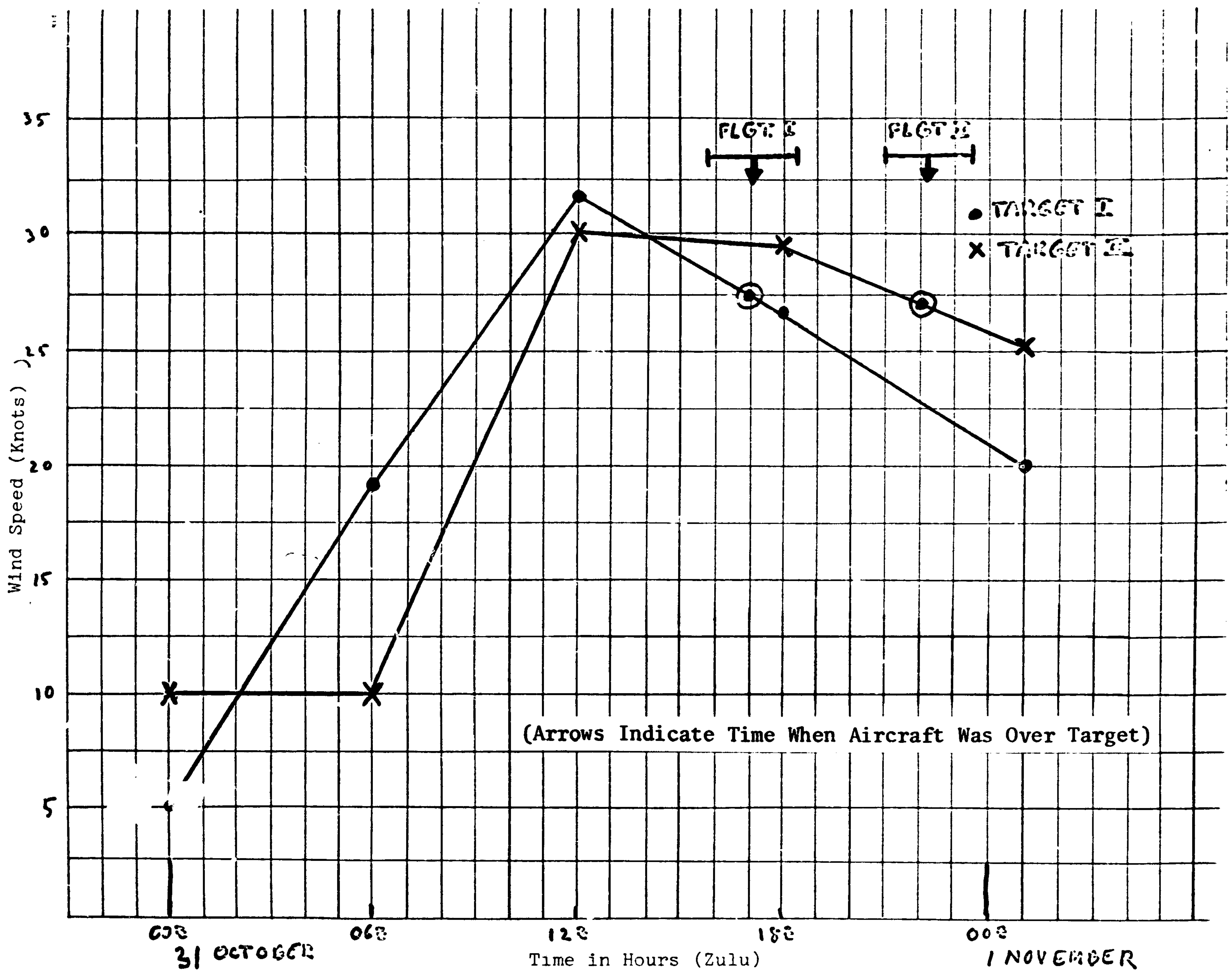

Figure 2-8 Wind Speed Versus Time at Targets I and II

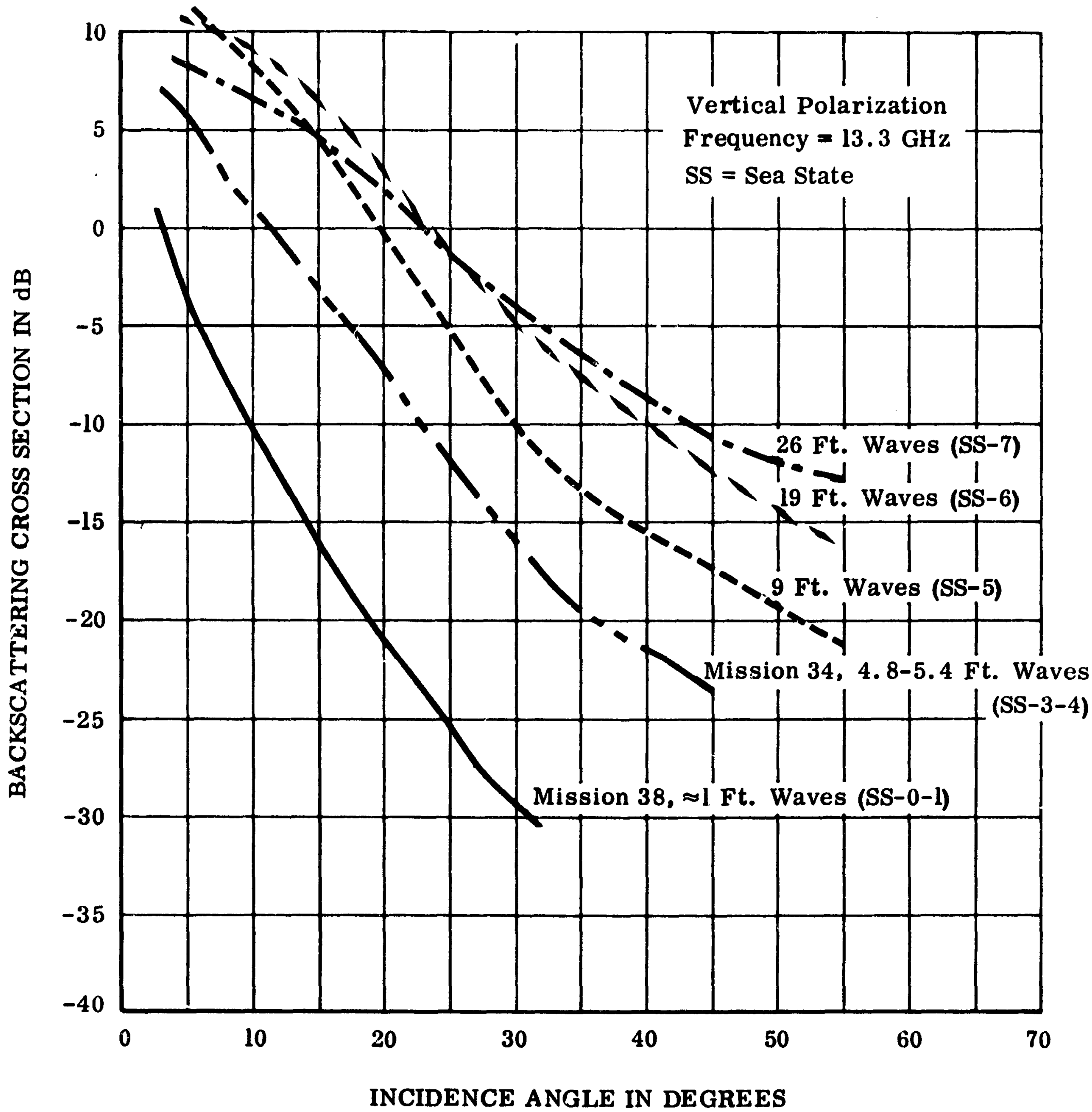

Figure 2-9 REDOP Scatterometer Response to Varying Sea State

SECTION 3

DIGITAL COMPUTER PROGRAMS

This section describes various computer programs developed for reduction of scatterometer data (13.3 GHz and 400 MHz).

3.1 ADVANCED REFLECTIVITY PROGRAMS

These programs utilize flight parameters and the radar backscattering equations to generate the scatterometer reflectivity data. Two additional programs were needed to arrange the flight information obtained from the photo panel to a format readily accessable and acceptable, and to calculate the time intervals of the requested data angles. The TIMTAB program indexes the appropriate flight parameters needed for proper reduction of data. A third program digitally filtered the entire frequency spectrum and selected data from discrete frequency bandwidths and placed these values on a digital tape for use on the last program. The fourth program is appropriately referred to as the REFLECT program, a complex data handling program. In addition to correcting for all of the system variables, it has the capability of generating radar backscattering cross section, time history curves and cross-correlation plots.

Conversion of the photo panel data from punched IBM cards to ASQ-90 format is accomplished by the NATRESOO program. This program also computes the necessary center frequencies and bandwidths required for digital filtering. The parameters are computed and tabulated on a listing for further use. A diagram of this program is shown in Figure 3-1.

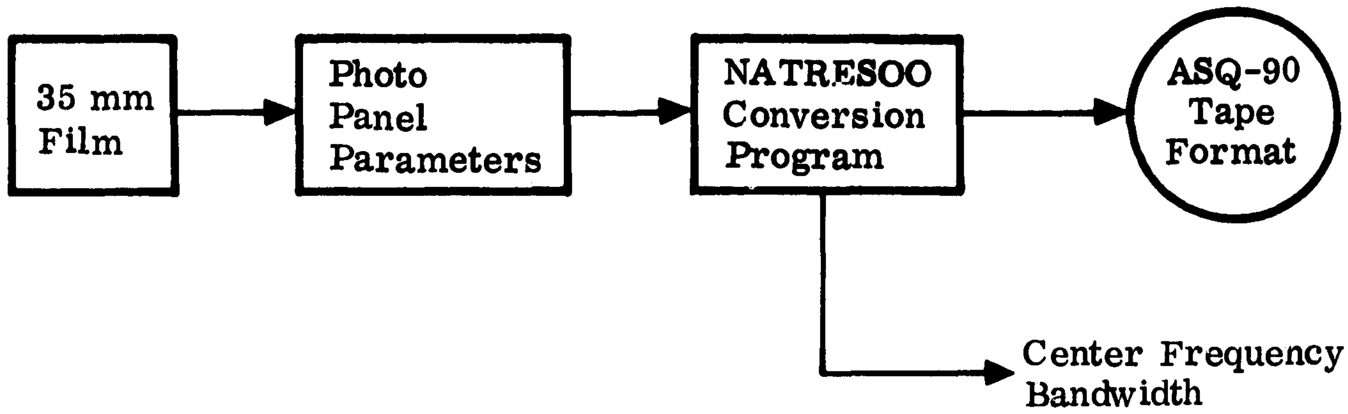

Figure 3-1 Photo Panel Film Conversion

The program TIMTAB (Figure 3-2) calculates the necessary time increments and cell interest times, which correspond to the requested angles of observation. After these time functions are calculated, flight parameters are time-indexed to be coincident. The flight parameters are then available to the REFLECT program, which computes the radar backscattering cross-section per unit area.

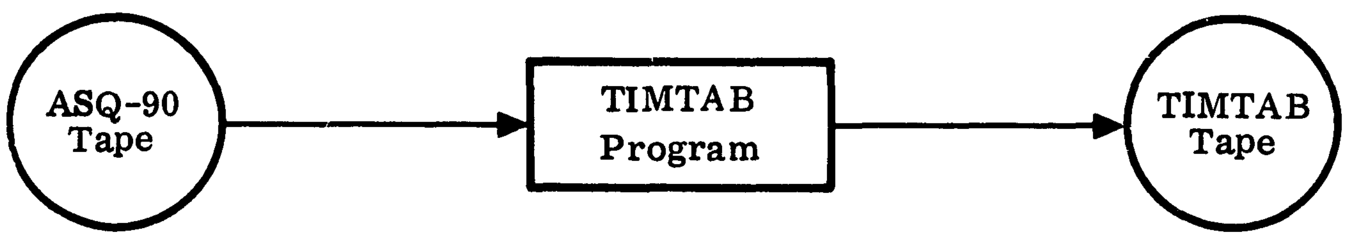

Figure 3-2 Time Table Calculations

The advanced computer program, REFLECT, (Figure 3-3) assumes the following conditions are available.

1. ASQ-90 data is available on tape at 1/10-second or 1/14-second intervals and includes at least ground speed, barometric altitude, radar altitude, roll angle, pitch angle and drift angle.

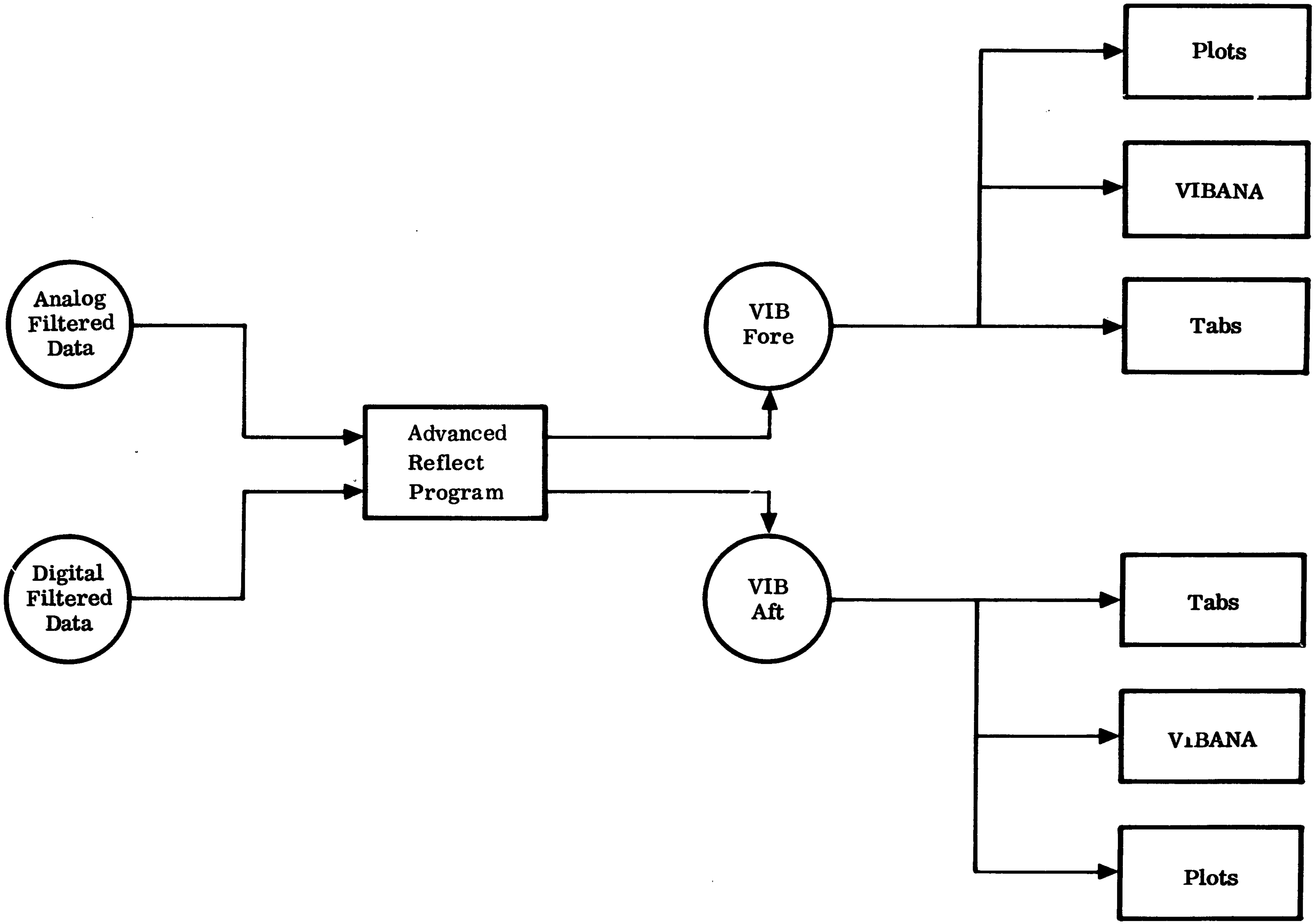

Figure 3-3 REFLECT Program

2. The Radar analog data tape has 11 channels including a 10 kHz reference channel, nine separate incident angle channels, and one IRIG time channel.

3. The Radar digital data tape produced from analog data tape includes multiplexed data from the 10 kHz reference and nine incident angle channels. Digital data is recorded such that each of the 10 channels will be equally represented. Each record is time coded with the time data on the analog data tape.

4. Basic inputs:

   a. Timetab Data Tape - these have data at 1/10 second intervals.

   b. Radar Data Tapes - "Phase I" format (digital tape with standard format).

5. Output - (SC-40-20 film)

   a. Radar reflectivity plots of backscattering coefficient (σ_o) in dB vs incident angle (θ).

   b. Statistical outputs for stated time intervals. The standard deviation of the averaged data are calculated and plots of average plus and minus one standard deviation are placed on the same grid with the average plot, a total of three plots occur on one grid.

   c. Time history plots of σ_o corrected for system and aircraft flight dynamic parameters.

   d. Auto correlation functions and curves.

   e. Power signal density curves.

Figure 3-4 A, B, C are representative samples of scatterometer data outputs available in graphic form from these computer programs.

3.2 DIGITAL FILTERING PROGRAM

The data reduction process for obtaining scatterometer data is playing magnetic tapes through a bank of parallel frequency filters which produces analog information in amplitude form. The center frequency of each filter corresponds to a specified incidence angle in accordance with the doppler relation between incidence angle and frequency: $D = \frac{2V}{\lambda} \sin \theta$, where D is the doppler frequency, V is the aircraft velocity, λ is the transmitted wavelength and θ is the incidence angle (measured from the nadir). The bandwidth of each frequency filter is proportional to the dimensions of the ground cell to be investigated. These cells are fixed in the broadside dimension by the angular antenna beam width, but variable in the longitudinal direction by center frequency bandwidth.

A request was made to develop a program for digitally filtering scatterometer data to replace the above analog system. The purposes for the digital filtering program were faster data turn-around, lower data reduction costs, and increased ability to handle quantities of data. The computer program is used in essence to generate a series of filters which extract spectral power density at each specified frequency band. These values are recorded on a digital tape and are used on conjunction with another computer program to produce σ_o values as a function of incidence angle. The center frequency and bandwidth of each filter is determined from aircraft velocity and altitude. Incorporation of digitally filtered data into the program should greatly increase accuracy and the number of data points available for each curve.

The 13.3 GHz scatterometer data is recorded on two tracks of analog tape from which a duplicate is generated and the original archived. This data is digitized using a CDC 3200 computer at 50 KHz (25 KHz per track). The

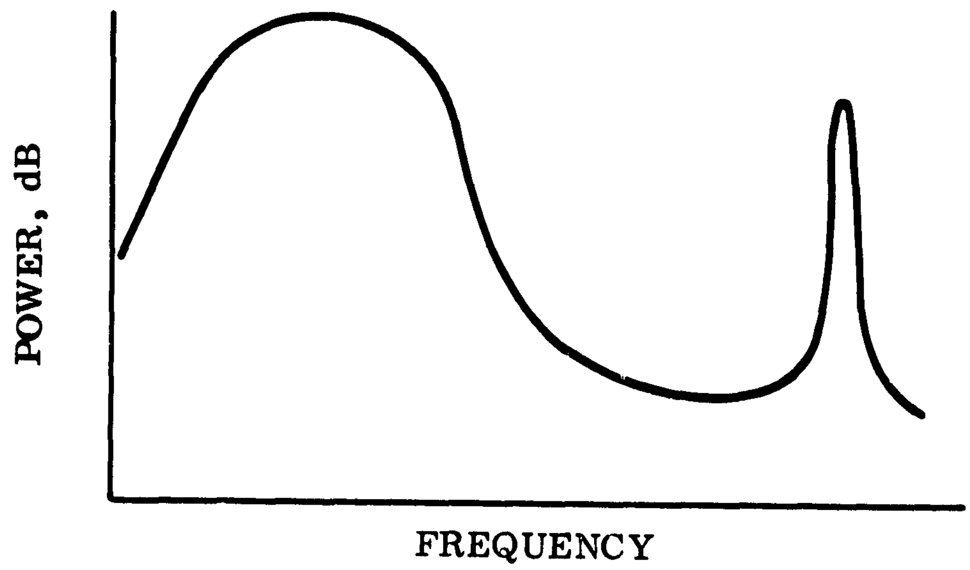

A. Power Spectral Density Plot

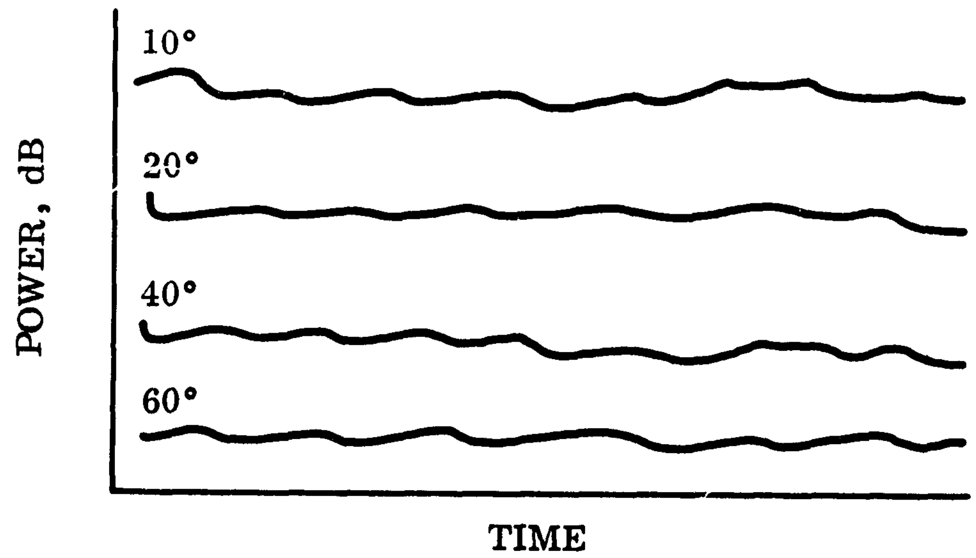

B. Time History Plot

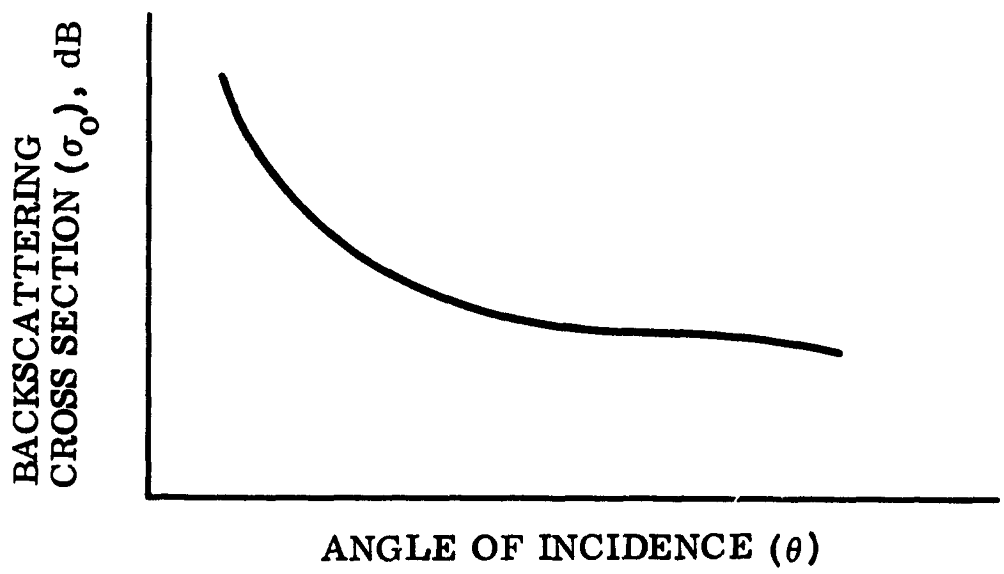

C. Backscattering Cross Section Versus Angle of Incidence Plot

Figure 3-4 Basic Reflectivity Data Forms entire frequency spectrum of amplitude versus frequency is solved by transforming sets of data value, up to 8192 points at a time, using a Fast Fourier Transform subroutine.

Figures 3-5 and 3-6 are block diagrams of the 13.3 GHz and the 400 MHz scatterometer digital filtering procedures. The analog information is digitized at a rate slightly higher than twice the highest frequency contained in the spectrum. Twenty KHz is not sufficient for the 13.3 GHz system due to biasing errors; therefore, a twenty-five KHz digitizing capability was developed. The data is read into the digital filter program at 25 KHz per channel and interpolated to 100 KHz. The digitized data is then sign-sensed and digitally filtered. The sign sense process (fore-aft beam designation) is effectively a single sideband modulator that shifts the doppler frequency to an intermediate frequency. The fore-beam data is at a higher doppler frequency than the IF and the aft beam data is at a lower doppler frequency. The IF base frequency is 20 KHz.

Digitally filtered data from missions 39 and 60 was compared to analog filtered data from the same flight, line and run. The digitally filtered data with a 40 KHz digitizing rate was continuously 5 to 6 db higher than the analog data. The digital data was hanned to eliminate the possibility of filter leakage by slope clipping the filter skirts. This technique has little effect on the reflectivity curves and merely reduces the amplitude of both data and reference signal. Maling[3] et. al. (1967) shows that hanning produces a nominal loss (for sine wave signals) of 4.26 db due to the generation of voltage sidebands, with the exact amount dependent on phase. It was, therefore, decided that only the filtered data be hanned. Hence, the possibility of introducing further errors by hanning the reference signal is eliminated.

The reference signal spectrum plot was later found to contain two peaks and numerous sidebands which were erroneously biasing the digitally filtered data. The phantom frequency spectrum above 10 KHz was a mirror image of

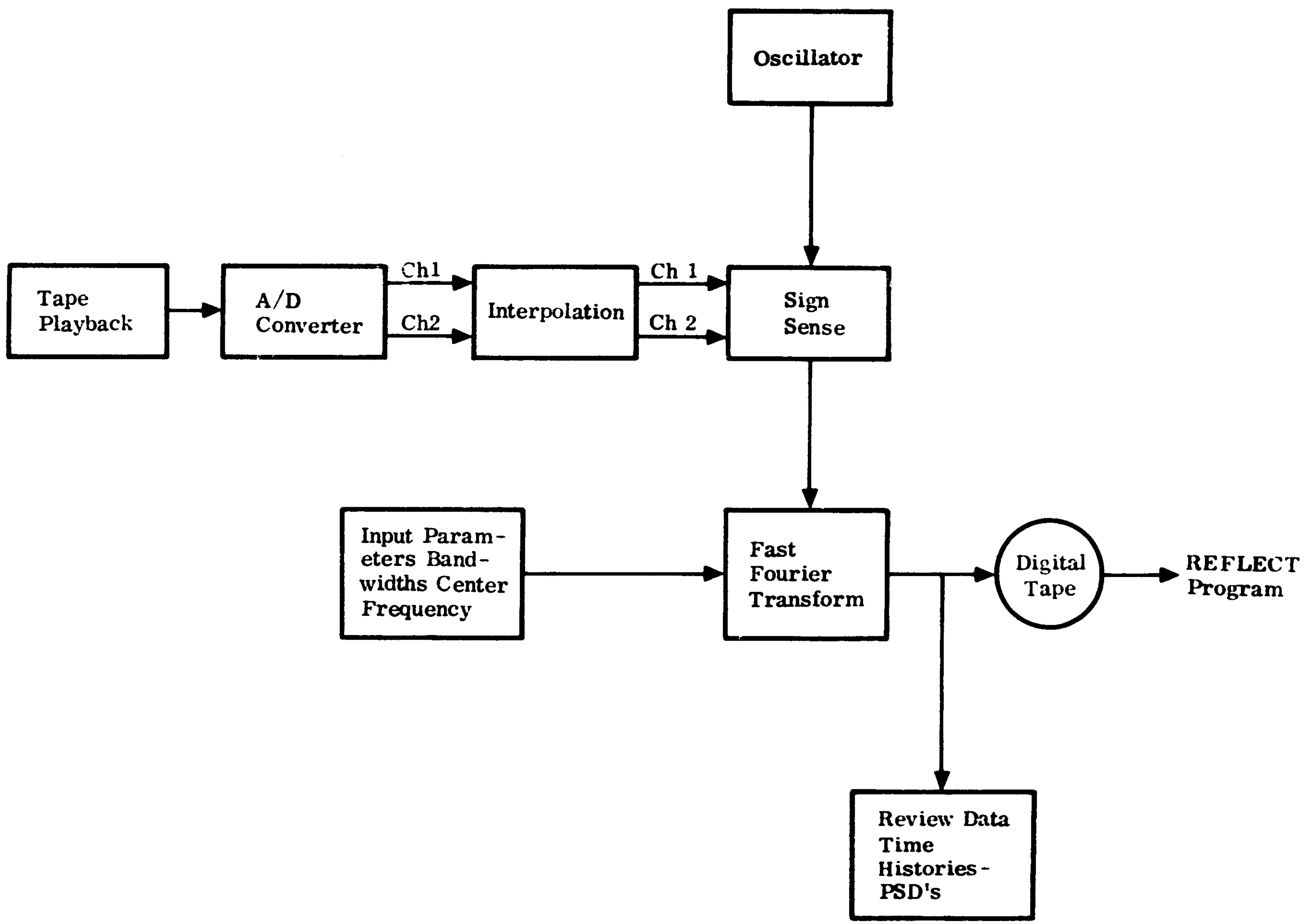

Figure 3-5 13.3 GHz Digital Filtering Program Block Diagram

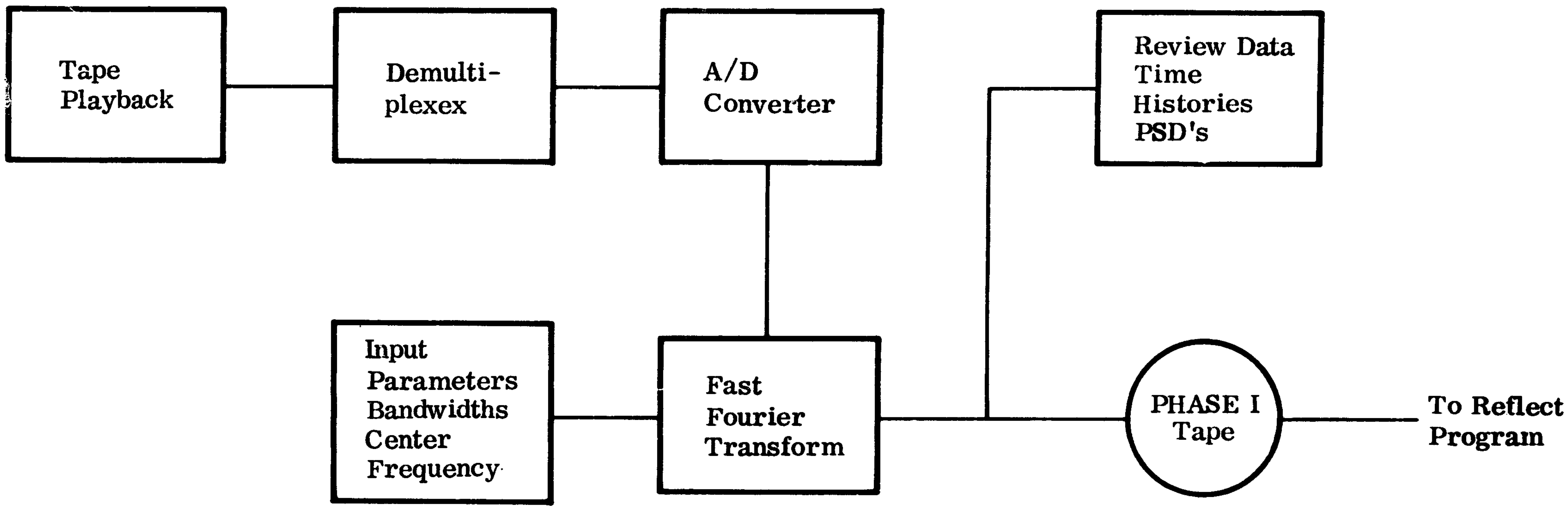

Figure 3-6 400 MHz Digital Filtering Program Block Diagram the real spectrum below 10 KHz, which is a well-known phenomena of sampling (see Cochran[4] et. al. 1967). The unwanted information above 10 KHz was effectively eliminated by sampling at a higher rate (50 KHz).

A program to increase the digitizing rate to 50 KHz (25 KHz per channel) is complete and operational. The results are within ±1.0 db of the previously verified analog results.

SECTION 4

SPATIALLY ADJUSTED TIME HISTORY TECHNIQUES

After studying the basic data forms used in displaying reflectivity information, it becomes obvious that the key to achieving a particular goal through analysis of terrain reflectivity lies in the choice of the appropriate data format from which the desired information can be gleaned most efficiently.

Analysis of the specific problems and goals associated with various Earth Resources studies has prompted the development of a data package designed especially for use by those investigators whose primary interest lie in Earth Resources.

A scaled version of such a proposed data package is shown in Figure 4-1. Forming the basis of this particular format is an "adjusted" time history plot. The plot has been redrawn so that the bottom scale is distance rather than time. This is done by shifting the information from the various incidence angles so that they line up spatially. This data format is called a Spatially Adjusted Time History (SATH) plot. A vertical line through the data, therefore, will yield the relative signal amplitude received from a specific spot of terrain. When correlated with aerial photos as shown, any spot of terrain within resolution limits, can be isolated and associated with its particular reflectivity pattern.

The SATH format is flexible since, with only slight modification, it can be used for other remote sensor data. Its continuous nature provides an accurate radar signature of an entire flight line. Also, due to the relationship between doppler frequency and incidence angle, the choice of angles to be plotted is a continuous function from -60° to +60°.

These plots can be obtained directly from the digital filtering program. A simple modification will be made to time shift each angle as it is plotted. Photographs are usually available for all flights so that visual correlations can be made, and the areas of interest labeled, prior to releasing the information through the Test and Operations Office. Radar altitude and velocity plots will be included with each package, making it possible to correlate the data with these parameters as they vary along the flight line.

In its broadest sense, the SATH technique of data presentation is based on pattern recognition. The simplest approach is to note the characteristics of the power return plot and "construct" the surface from basic reflectivity theory. For example, the power level increases rapidly at the higher incidence angles between 8500 and 9000 feet, down the track, (Figure 4-1), showing the terrain has relatively changed from smooth to rough. Return from angles near the nadir reinforces this conjecture by following, in opposite phase, the data from the higher angles. Therefore, with no other ancillary information, it is possible to identify terrain characteristics.

By applying this pattern recognition technique the plot in Figure 4-1 was divided into several areas on the basis of characteristic reflectivity variations. The areas were correlated with ground truth data and classified such categories as ground truth data and classified such categories as vegetated desert (A), old river bed (B), sparsley vegetated rough desert (C), drainage ravine (D), smooth desert sand (E) and rough lava (F). The lines of correlation are only approximate because the aircraft path was assumed to be a straight line. In future work the aircraft dynamics will be incorporated such that a beam path closely approximating the true ground track will be displayed. In this manner lineations such as the northeast-southwest alinement in the lower center portion of the photograph may be more realistically correlated with scatterometer return signatures.

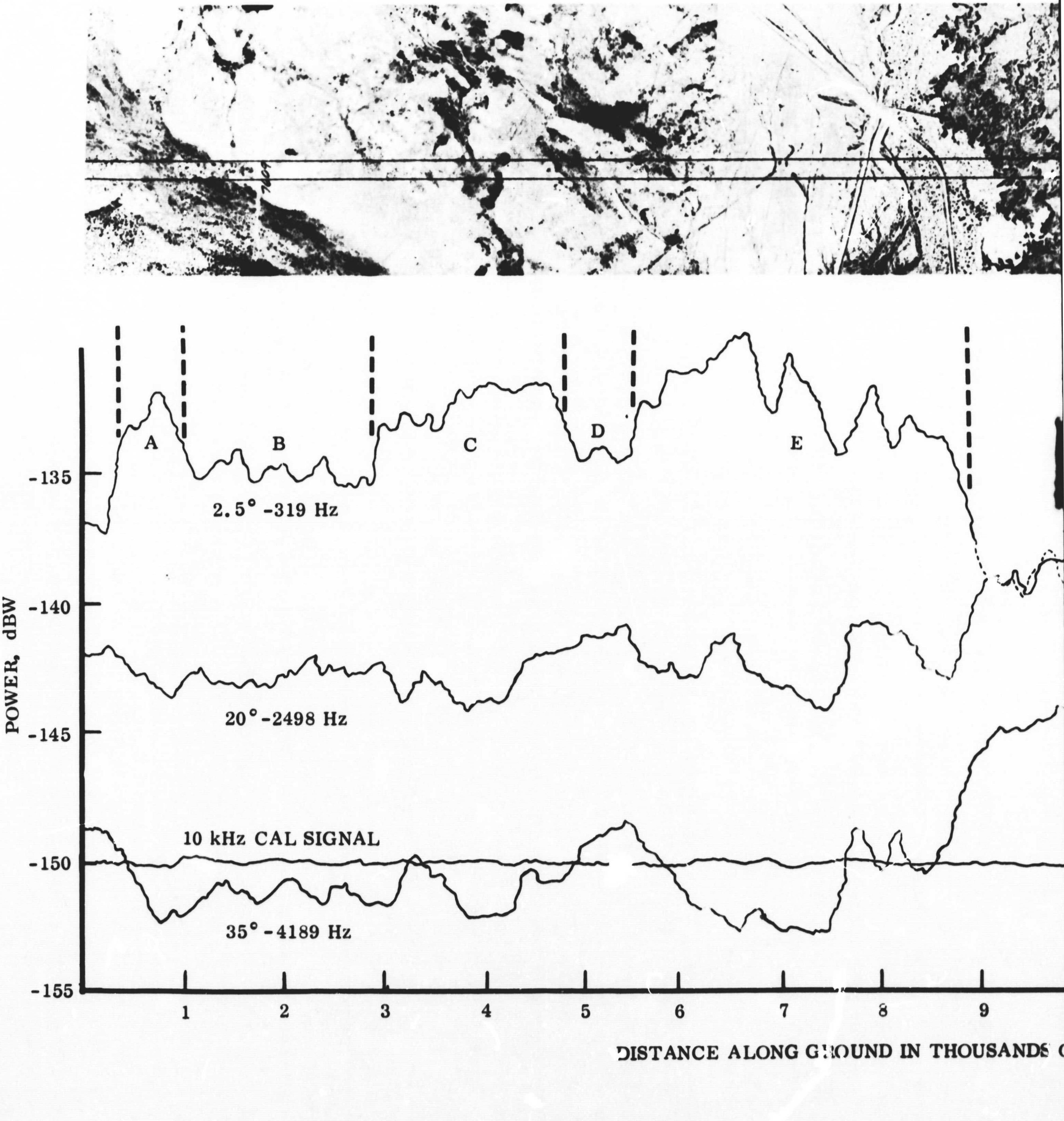

Figu

FOLDOUT FRAME 1

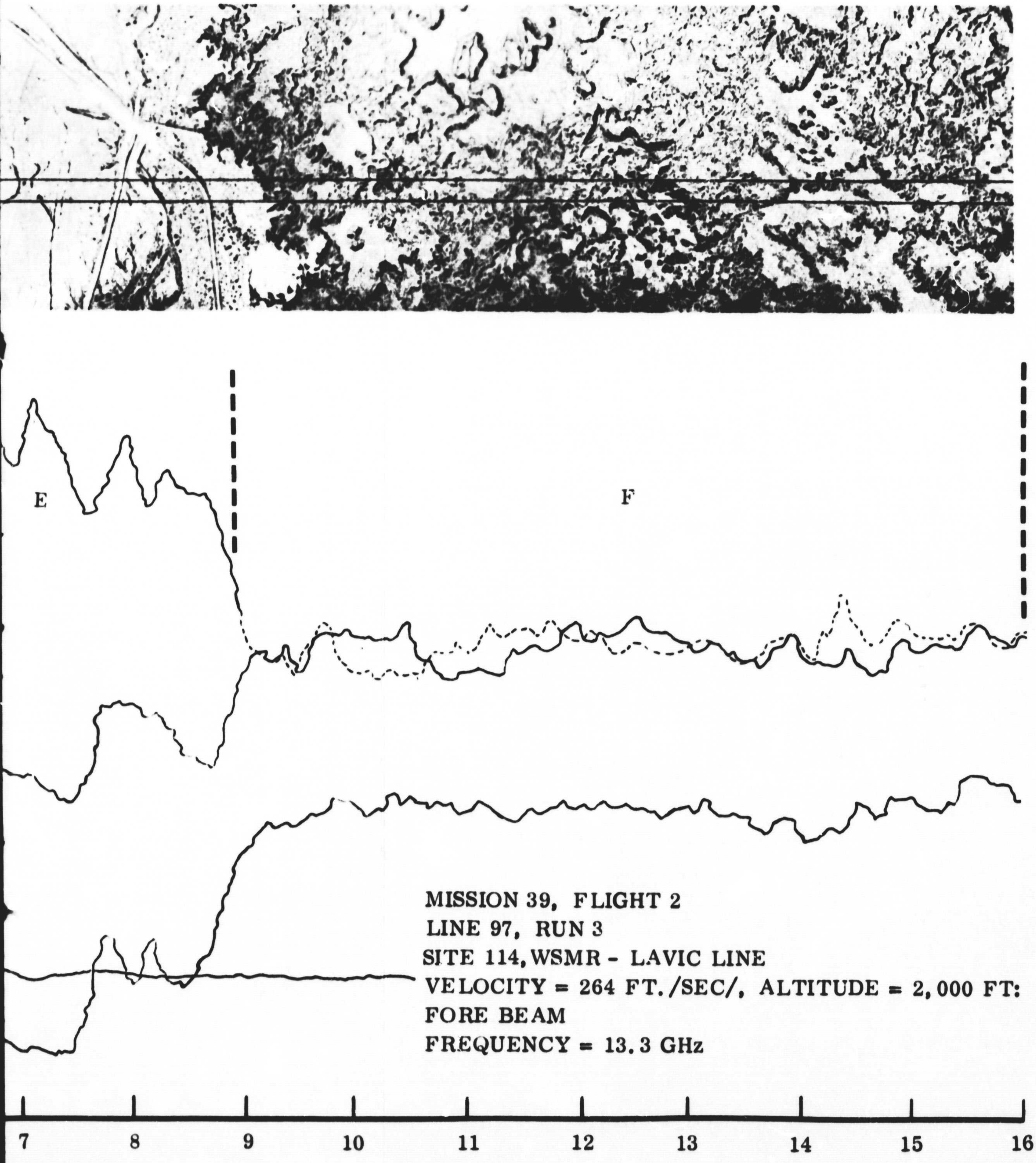

Figure 4-1 Representative SATH Plot

FOLDOUT FRAME 2

While the information being sought may be present in the remote sensor data under investigation, without the proper format for presentation of output, it may not be possible to extract the desired results. Therefore the choice of such a format is an important part of any remote sensor data analysis program. The SATH format has been studied and found to be quite useful in Earth Resources study and refinement of this technique is being carried out at present. It is felt that to remove the possibility of errors due to system or aircraft parameters, the data should be reduced to the corrected σ_o form then plotted in SATH format. The data would then be completely adjusted and points could be read directly from the plots to yield σ_o versus θ curves for each particular terrain feature. This is one of the many possibilities which are now under investigation.

SECTION 5

A DISCUSSION OF MATHEMATICAL MODELS

Because of the complexity of a backscattering surface, either for land or sea, a number of different models have been proposed by various researchers. The reason for developing a mathematical model is to provide a tool for analyzing the scattering mechanism in terms of terrain characteristics. Because of the many different approaches used in such development, one should expect each model to be limited to those conditions under which their initial assumptions may be considered valid. Perhaps the most important of these conditions is the model of surface roughness for which the theory was developed.

As a part of the Scatterometer Data Analysis Program, various models are being investigated to see how well the differences in radar backscattering can be predicted. The procedure presently used is to obtain curve fits with a mathematical model and then to compare the model-predicted surface parameters with actual measurements of the terrain surface parameters. If experimental data fits a theoretical model, prediction of survey results can be anticipated.

Many theoretical models of the backscattering surface have been proposed in the past to describe the scattering mechanisms of a rough surface. Under limited conditions, these models were able to describe qualitatively the backscattering from some hypothetical rough surface. The authors, in almost all cases, pointed to the experimental data to obtain values for the parameters in the models. These models were, however, quite powerful in establishing some of the scattering mechanisms, or the nature of the mechanisms, and the expected forms for σ_o as a function of angle, frequency, facet size, polarization, etc. However, introduction of various parameters into these models, so that they could be used for establishing a one-to-one correspondence with known terrain types, showed the models to have shortcomings in nearly every case.

A brief survey of the statistical models (Davies[5], Moore and Hayre[6], Beckman[7] and Fung[8]) indicates that Fung's statistical model of power return for a scattering surface embodies all of the considerations on frequency and correlation. However, the postulate of a rather artificial correlation function containing many adjustable constants inevitably makes the result an empirical formula. Also, the curve-fitting process to evaluate the parameters becomes much more complicated. On the other hand, Beckmann's model, designed to explain the dependence of the mean backscattered power on the angle of incidence, shows that this dependence may be derived without any artificial assumptions.

Beckmann's model suggests that the major contribution to the amplitude of backscattered signals are not necessarily from those components of largest size and angularities, but from surface irregularities that present the highest RMS slope (σ/L) values. The statistical models of rough surfaces by Davies, Moore and Hayre treat the height variation by a single statistical distribution and a single correlation function. Rough surfaces in nature, however, are in essence composite structures, or better can be treated as such. A rough surface(s), according to Beckmann, can be described by a superposition of j random variables:

$$\delta(x, y) = \delta_1 (x, y) + \delta_2 (x, y) + \dots .$$

each having its own statistical distribution and correlation function. Therefore, the model considers the return due to both large and small scale scatterers. For example, rolling hills would be considered a large-scale scatterer; whereas, plowed fields, sandy surfaces and grass would be considered as small-scale scatterers.

Two statistical models were developed by Beckmann for random rough surfaces which were applied to the special case of backscattering. One model used a general analytical function and the other an exponential form. The mean power P_R backscattered as derived from the analytic correlation function is:

$$P_R = P_o \cos^{-4}\theta \; e^{-Q \tan^2\theta} \; S(\theta) \qquad (1)$$

where $P_o = \dfrac{E_o^{\,2}\,\lambda^2 Q}{4\pi\eta A}$,

which is the mean power scattered in the specular direction (i.e., $\theta = 0$), and

$$E_o = \frac{KA}{\eta R_o}$$

$$Q = \frac{1}{2\sum_j s_j^2}$$

A = equivalent plane surface area

λ = wavelength

η = impedance of the medium of the incident side of the interface formed by a rough surface

R_o = distance to area element "A" at normal incidence

$S(\theta)$ = shadowing function

s = σ/L where σ is the standard deviation of the element heights and L is a correlation distance between them

Since there is no contribution to the backscatter from the shaded areas, it is necessary to multiply the equation by the shadowing function which is equal to,

$$S(\theta) = \exp\left[-\frac{1}{4}\tan\theta \; \mathrm{erfc}\;(K \cot\theta)\right] \qquad (2)$$

where K is defined by $K = \sqrt{Q}$

The mean power P_R' backscattered as derived from the exponential correlation function is:

$$P_r' = P_o \left(\cos^4\theta + R \sin^2\theta \right)^{-3/2} S(\theta) \qquad (3)$$

where

$$P_o' = \frac{E_o^2 \lambda^2 R}{8\pi\eta A}$$

and

$$R = \frac{1}{\left(4\pi \sum_j r_j s_j\right)^2}$$

where

$$r = \sigma/\lambda$$

Examination of equations (1) and (3) clearly indicates that the dependence of the mean backscattered power on θ is determined by the values of Q and R. In both cases it will usually be the small-scale components of the surface which will contribute largely to Q and R. Figure 5-1 illustrates the curve fit with Beckmann's model when compared to data taken with a 13.3 GHz scatterometer of a desert with dunes.

Moore and Pierson[9] (1965) discuss two basic correlation functions; the Gaussian or analytic function and the exponential function. The Gaussian function is:

$$\rho(\xi) = e^{-\xi^2/L^2}$$

with ξ the horizontal distance between points being correlated and L a scale distance. Examples of this form can be found in publications by Davies[9] (1954), Janza[10] (1963), and Moore[11] (1957). (See Table 5-1.) Figure 5-2 shows the curves that are expected from these models. Hayre's model was developed using an exponential correlation function:

$$\rho(\xi) = e^{-|\xi|/L}$$

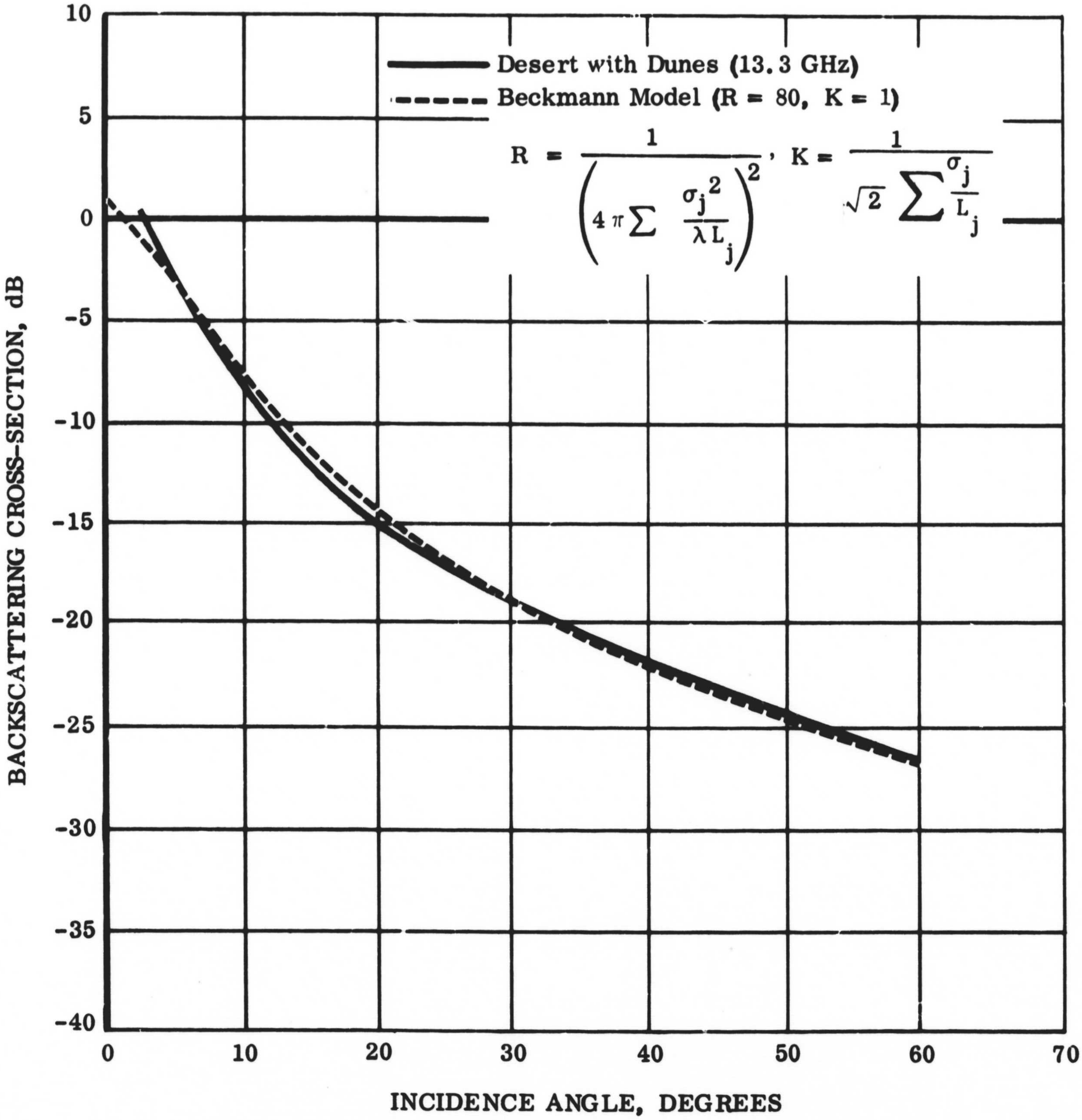

Figure 5-1 A Comparison of Beckmann's Model with Measured Data

Table 5-1 Example Equations

$$\sigma_o = \frac{L^2}{4\sigma^2} \exp - \frac{L^2}{2\sigma^2} \tan^2 \theta \qquad \text{(Davies-Analytic)}$$

$$\sigma_o = k^2 \frac{L^2}{2\sigma^2} \exp - \frac{L^2}{2\sigma^2} \tan^2 \theta \qquad \text{(Janza-Analytic)}$$

$$\sigma_o \approx \frac{L^2}{2\pi\sigma^2} \theta \csc\theta \exp - \frac{L^2}{2\sigma^2} \tan^2 \theta \qquad \text{(Moore-Analytic)}$$

$$\sigma_o = 4\pi \sqrt{2} \left(\frac{L}{\lambda}\right)^2 \left(\frac{\theta \cos^2\theta}{\sin\theta}\right) X \qquad \text{(Hayre-Exponential)}$$

$$\exp - 4k^2 \sigma^2 \cos^2 \theta \sum_{n=1}^{\infty} \frac{(4k^2 \sigma^2 \cos^2\theta)^n}{(n-1)! \left[2L^2k^2 \sin^2\theta + n^2\right]^{3/2}}$$

L = effective correlation length between scattering ground elements identified with a wavelength scale size.

σ = standard deviation of the surface height variations about a mean level.

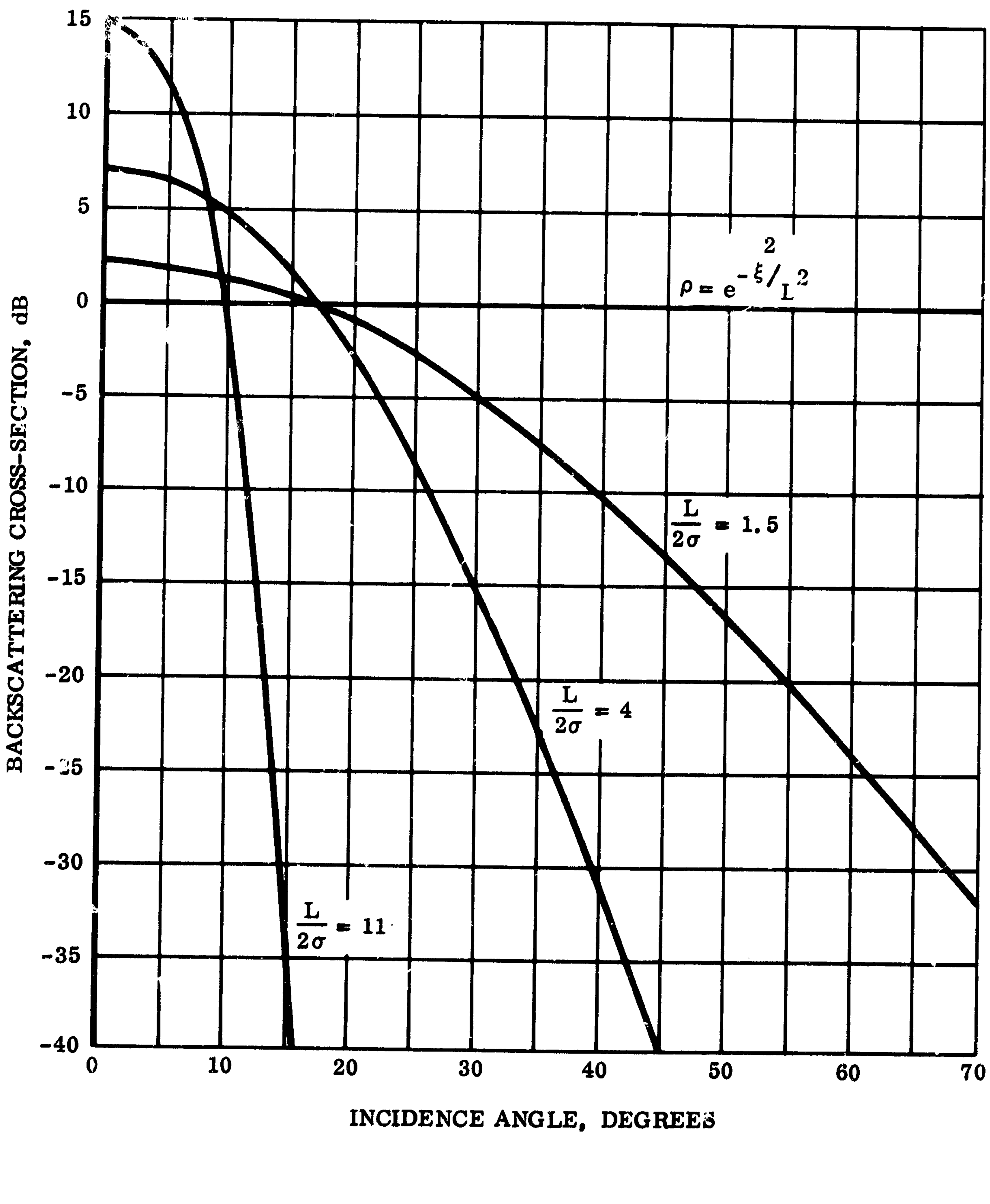

Figure 5-2 Analytic Correlation Function (Moore and Pierson 1965)

To supplement these studies, additional ground correlation measurements will be required. Emphasis should be placed on isolating and measuring the specific parameters, such as σ and L, in the near future. Other important parameters such as the dielectric and conductive properties have not been determined for a sufficient number of materials to indicate their contribution to modeling formulas. Knowledge of the type of data being obtained from sensors is a prerequisite for determining those terrain parameters which will have the greatest affect on data. Thus, data can be most efficiently gathered by teams familiar with the Earth Resources Remote Sensors Program.

SECTION 6

400 MHz SCATTEROMETER DATA REDUCTION SYSTEM

The objective of the program is to measure the radar backscattering cross-section per unit surface area, σ_o as a function of incidence angle θ using a scatterometer operating at a frequency of 400 MHz and the comparison of data with that obtained from the 13.3 GHz REDOP System. Because of the long wavelength associated with a 400 MHz system and its greater sensitivity to large surface structures, the system will be used to investigate relatively large scale structural features for oceanography, geology, and general land surveys. This data along with data taken with the 13.3 GHz scatterometer with its greater sensitivity to small surface structures, should yield valuable additional information concerning surface configurations. Such information can be processed with applicable techniques and correlated with ground information to establish utility.

6.1 400 MHz SCATTEROMETER OUTPUTS

Four outputs from each receiver front end are processed in separate channels consisting of a fixed end and a variable gate resulting in a total of eight signals. Airborne processing will consist of recording the eight signals, along with a calibrate channel, on a single track of magnetic tape. During post-flight data processing the output from the recorder playback unit is demultiplexed to obtain the nine data channels. This data is then digitally filtered and computer processed to yield the desired σ_o versus θ plots.

6.2 DYNAMIC RANGE CONSIDERATIONS

An important physical constraint in this type of system is the dynamic range variation in received signal level. The maximum range of σ_o is 65 db plus 18 db fading, 6 db for the change in slant range, and 32 db for changes in altitude, a total variation in received signal amplitude of 121 db.

Therefore, it becomes necessary to use techniques for reducing the dynamic range to values that are compatible with the AR-1600 tape recorder. These include antenna beam shaping, manual gain adjustment, automatic gain control, and variable time gating.

Antenna beam shaping can be used to reduce the signals returned from near nadir and enhance signals returned from larger incidence angles. However, the 400 MHz system is limited to a single pattern, which is not ideal for use over various terrain because the signal return is a function of terrain. The requiremonts can best be seen by examing the bandwidth of the data and the radar equation in the following form:

$$G_o^2(\theta)f'(\theta) = \frac{KW_sR^2\cos^2\theta}{\sigma_o(\theta)}$$

where

$G_o^2(\theta)f'(\theta)$ = two-way antenna pattern factor

K = constant

W_s = signal power density

R = range

$\sigma_o(\theta)$ = backscattering cross section per unit area

Holding signal power density constant the equation can be rewritten:

$$G_o^2(\theta)f'(\theta) = \frac{K_1R^2\cos^2\theta}{\sigma_o(\theta)} = \frac{K_1h^2}{\sigma_o(\theta)}$$

where

$K_1 = KW_s$

$h = R\cos\theta$ = radar altitude

The previous equation establishes the inverse relationship of $\sigma_o(\theta)$ and $f'(\theta)$, that is, the value of the two-way antenna pattern factor is a maximum for minimum $\sigma_o(\theta)$ values. Because of the tape recorder dynamic range limitation, this value should be reduced by:

$$G_o^2(\theta) f'(\theta) = \frac{k_1 h^2}{\sigma_o(\theta)} - \text{(dynamic range of tape recorder)}$$

Manual and automatic gain control can be effective in reducing the dynamic range requirement due to altitude changes. Manual gain control can reduce the dynamic range by allowing the operator to compensate each receiver for altitude and total reflectivity changes. Automatic gain controls within each receiver adjusts the output of the receiver to a level compatible with the AR-1600 tape recorder.

By incorporating variable time gating and four additional receiver channels the overall dynamic range of the system can be increased. Using fixed gate channels, the AR-1600 system can record the spectral return with a 40 db dynamic range. However, this range is only good for the lower incidence angles. To increase the range and accept the data beyond this point, the leading edge of the variable gate can be adjusted until the strong returns are reduced. This additional attenuation, introduced by the adjustable time delay, increases the total dynamic range capabilities of the system.

6.3 SIGNAL-TO-NOISE COMPUTATION

Theoretical studies for the 400 MHz system in conjunction with surface reflectivity characteristics can be found by the derivation and analysis of equations relating system parameters and backscattering cross section per unit surface area. Deriving such equations starts with those involving signal return from the scattering surface.

The power density of incident radiation at the surface of the earth, S^i, may be expressed in terms of antenna characteristics G(q); transmitted power, P_t, and range, R, as follows:

$$S^i = \frac{P_t}{4\pi R^2} G(q)$$

where the quantity $P_t/4\pi R^2$ is the power density which would result from isotropic radiation of transmitted power and G(q) is the power gain of the antenna over the gain of an isotropic radiator in a direction determined by the space coordinate, q, measured from the beam axis. The antenna gain, G(q) may be written in terms of its maximum value, G_o, and a pattern factor, f(q) as follows:

$$G(q) = G_o f(q)$$

Backscattered power density, S^s, from a single scattering element is related to incident power density by

$$S^s = S^i \frac{\sigma}{4\pi R^2}$$

where the backscattering cross section, σ, is defined as the isotropic scattering area normal to the axis of the beam which produces an echo equal to that observed from the target when illuminated by the same incident power density.

Earth's surface areas may be assumed to consist of a number of independent scattering elements. It is convenient to define the quantity $\sigma_o(\theta)$ as the average backscattering cross section per unit surface area:

$$\sigma = \int \sigma_o(\theta)da$$

where the integration is over the illuminated region.

The differential backscattered power density from an incremental surface area, da, having an angle of incidence θ becomes,

$$dS^s = S^i \frac{\sigma_o(\theta)da}{4\pi R^2}$$

The echo power received is related to backscattered power density and to the effective receiving area of the antenna, A_e:

$$P_R = A_e S^s$$

The effective receiving area, A_e, may be written in terms of antenna gain and the wavelength of the radiation:

$$A_e = \frac{G_o f(q)\lambda^2}{4\pi}$$

The differential scattered power received per incremental surface area becomes

$$dP_R = A_e dS^s = \frac{P_t G_o{}^2 [f(q)]^2 \lambda^2 \sigma_o(\theta) da}{(4\pi)^3 R^4}$$

The antenna pattern factor, expressed in terms of the beam coordinates θ and φ, is:

$$[f(q)]^{-2} = f_1(\theta,\phi)$$

where $f_1(\theta, \phi)$ is the two-way antenna pattern factor. The differential surface area, da, may also be expressed in terms of the coordinates θ and φ, and the range to the surface R.

$$da = \frac{R^2}{\cos\theta} d\theta d\phi$$

The amount of power received from an incremental area on the surface bounded by the angles $\theta_o - \frac{\Delta\theta}{2}$ to $\theta_o + \frac{\Delta\theta}{2}$ and $\phi - \frac{\pi}{2}$ to $\phi + \frac{\pi}{2}$ becomes:

$$\Delta P_R = \frac{P_t G_o^{2} \lambda^2}{(4\pi)^3} \int_{\theta_o - \Delta\theta/2}^{\theta_o + \Delta\theta/2} \frac{\sigma_o(\theta)}{R^2 \cos\theta} \left[\int_{-\pi/2}^{\pi/2} f_1(\theta, \phi)\, d\phi \right] d\theta$$

The amount of received power, as a function of frequency, can be obtained by substituting an equivalent increment of frequency for the angular increment, $\Delta\theta$. The doppler frequency, f, can then be expressed by;

$$f = \frac{2V}{\lambda} \sin \theta,$$

where V is the velocity of the antenna with respect to the surface of the earth, and

$$\frac{df}{d\theta} = \frac{2V}{\lambda} \cos \theta, \qquad \frac{d\theta}{df} = \frac{\lambda}{2V \cos \theta}$$

An angular increment of $\frac{\lambda}{2V \cos \theta}$ radians is equivalent to a frequency increment of 1 Hz.

Considering a wide fore-aft beam antenna, $f_1(\theta, \phi)$ that is a slowly varying function of θ:

$$\int_{-\pi/2}^{\pi/2} f_1(\theta,\phi)\, d\phi = f_2(\theta) B_\phi$$

where B_ϕ is the lateral antenna beamwidth. The integral over θ covers the incremental range $\Delta\theta$ and becomes:

$$B_\phi \int_{\theta_o - \Delta\theta/2}^{\theta_o + \Delta\theta/2} \frac{\sigma_o(\theta) f_2(\theta) d\theta}{R^2 \cos\theta}$$

For small $\Delta\theta$:

$$\frac{B_\phi \sigma_o(\theta) f_2(\theta_o)}{R^2 \cos\theta_o} \int_{\theta_o - \Delta\theta/2}^{\theta_o + \Delta\theta/2} d\theta = \frac{B_\phi \sigma_o(\theta_o) f_2(\theta_o) \Delta\theta}{R^2 \cos\theta_o}$$

Substituting for $\Delta\theta$ that angular increment which gives a frequency increment of one Hz,

$$\frac{B_\phi \sigma_o(\theta_o) f_2(\theta_o) \lambda}{2VH^2}$$

The amount of echo power (W_{sa}) received at the antenna for an increment frequency of 1 Hz at $\theta = \theta_o$, may then be written:

$$(W_{sa}) = \frac{P_t G_o^2 f_2(\theta_o) \lambda^3 \sigma_o(\theta_o) B\phi}{2(4\pi)^3 VH^2}$$

When the system is operated as an interrupted continuous wave system the average power transmitted is $\delta_s P_t$ where δ_s is the ratio of the pulse width transmitted to the pulse repetition period. Of this transmitted power, only an amount δ_s is usable, the remainder is redistributed as harmonics of the pulse repetition frequency. Therefore, the relative power contained in the fundamental is $\delta_s^2 P_t$.

The power received has thus far been referred to the antenna terminals. When referred to the first IF amplifier input, the signal power level becomes:

$$(W_{si}) = \frac{P_T G^2(\theta) \lambda^3 \sigma_o(\theta) B_\phi \delta_s^2}{2(4\pi)^3 VH^2 L_s L_m}$$

where

L_s = switching loss

L_m = miscellaneous loss

$$G^2(\theta) = G_o^2 f_2(\theta)$$

where θ_o is generalized to θ.

The noise power density referred to the mixer output (including the IF noise contribution) is

$$W_{ni} = KTF\ \delta_n$$

where

= Boltzmann constant

= reference temperature (290 degrees K)

F = preamplifier noise figure

δ_n = receiver gated on duty cycle

The signal-to-noise power density ratio is:

$$\frac{W_{si}}{W_{ni}} = \frac{P_T G^2(\theta)\lambda^3 \sigma_o(\theta) B \delta_s^2}{2(4\pi)^3 V H^2\ L_s L_m\ KTF\ \delta_n}$$

The following example (Table 6-1) illustrates the signal-to-noise ratio calculation.

Table 6-1 Signal-to-Noise Ratio Calculation

(40,000 Ft. Alt., 60 degrees Incidence, - 40 db Reflection Coefficient)

Signal Power Density $W_s = \dfrac{P_t G^2(\theta)\lambda^3 B\delta_s^2\sigma_o(\theta)}{2(4\pi)^3\ VH^2\ L_s L_m}$ (dBW/Hz)

SYMBOL		VALUE (dB)
P_t	Transmitted Power (20 watts)	13.0 dBw
G^2	Antenna Gain (2-way, 60 degrees)	34.0
λ^3	Wavelength $(2.46\ \text{Ft.})^3$	11.7
B	Beamwidth (3 degrees in radians)	-12.8
δ_s^2	Duty Cycle (.302 or .151 per channel)	-16.4
σ_o	Backscattering Coefficient	-40.0
$1/2(4\pi)^3$	Constant	-36.0
$1/V$	Velocity (1/590 FPS)	-27.7
$1/H^2$	Altitude $(1/40{,}000\ \text{Ft.})^2$	-92.0
$1/L_s$	Switching Loss (estimate)	-1.5
$1/L_m$	Miscellaneous Losses (estimate)	-1.0
W_s	Signal Power Density (amplifier input)	-168.7 dBW

Noise Power Density = W_n = KTF δ_n

KT	Thermal Noise at 290 Degrees K	-204.0 dBW
F	IF Amplifier Noise Figure (estimate)	9.0
δ_n	Receiver Gated on Duty Cycle	-4.8
W_n	Noise Power Density (amplifier input)	-199.8 dBW
W_s/W_n	Signal-to-Noise Density Ratio	31.1

6.4 FUNCTIONAL DESCRIPTION

Figure 6-1 is a simplified block diagram of the 400 MHz scatterometer system. The horizontal (H) and vertical (V) receivers accept the reflected signal. They also receive inputs from the first local oscillator source (LO) and the calibrate source. The four output signals are applied to an IF switch which consists of a series of eight solid-state switches with built-in drivers. Gating signals for these switches are received from the synchronizer.

The eight signals are routed to eight post IF receivers. Each receiver obtains two other inputs generated by the low frequency source (LF). The output from each receiver is sent to a multiplexer and is recorded on the tape recorder. The output is also coupled to an AGC circuit with a meter for indicating signal strength.

Three input signals are applied to the calibrate source which provides a reference signal 500 Hz above the transmitter frequency. A 55 MHz signal and a 5.005 MHz signal are received from the LF source, while a 340 MHz input is obtained from the first LO source. Two of the three outputs from the calibrate source are alternately applied to the H and V receivers through an external RF transfer switch. This is to compensate for the greater signal level which appears in the receiver that is matched to the polarization of the transmitted signal. The third output is channeled directly to the calibrate receiver.

The first LO source receives a 5 and 55 MHz input from the LF source, and a 400.85 MHz input from the transmitter and supplies 340 MHz outputs to the calibrate source, calibrate receiver and the H and V receivers. The outputs to the H and V receivers are gated off during transmission.

The LF source generates its output signals from three oscillators operating at 500 Hz, 5 MHz and 55 MHz. An output signal from the 55 MHz oscillator is subdivided into nine parts for use as a local oscillator source in the eight post IF receivers and the calibrate receiver. In the same way, the

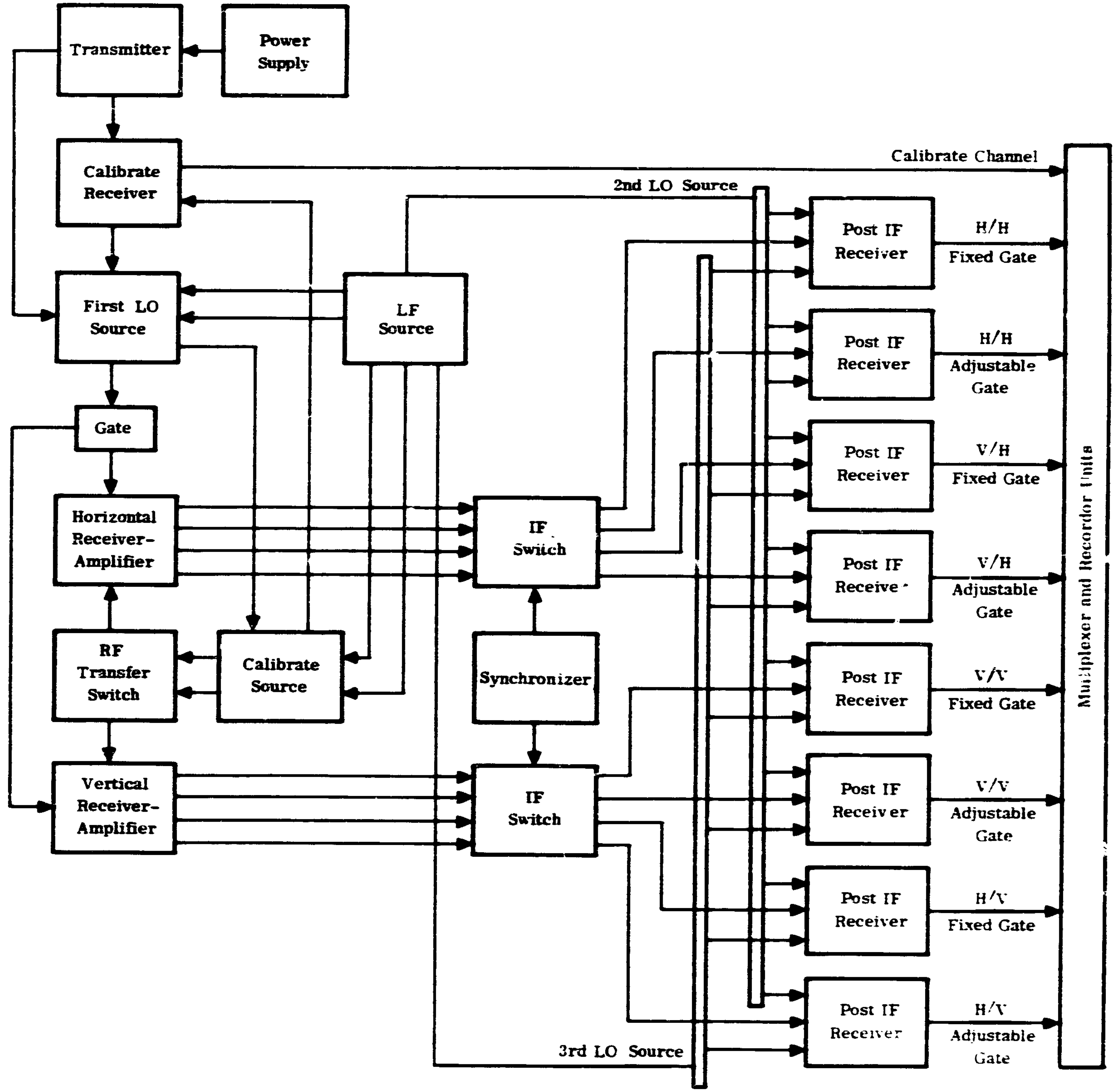

Figure 6-1 400 MHz Scatterometer Simplified Block Diagram

5 MHz oscillator is mixed with 500 Hz oscillator and applied to the post IF receivers as a second LO source. Four other outputs are available from the LF source. Two of these (one from the 55 MHz and another from the 5 MHz oscillator) go directly to the first LO source. A third signal at 55 MHz, is used by the calibrate source. The last signal, which is derived by mixing the 5 MHz and 500 Hz source, is also applied to the calibrate source.

6.5 DIGITAL COMPUTER PROGRAM MODIFICATIONS

The 400 MHz scatterometer is an ICW system with dual polarization. Therefore, data handling becomes more complex than for a single polarization 13.3 GHz system. An additional complication is use of a fixed and a variable receiver gate for each channel. The entire received spectrum is passed by the fixed gate with only a selected portion of the spectrum passed by the variable gate channels.

The equation for computing σ_0 for the 400 MHz system is similar to that used for the 13.3 GHz system. The 400 MHz system does incorporate correction factors for the duty cycle and switching loss. The following is a description of the 400 MHz program.

6.5.1 General Modifications

The 400 MHz scatterometer data recording system in its present configuration will enable investigators to recover any segment of data from any one of the eight data channels.

The eight 400 MHz scatterometer data channels and one calibrate channel recorded on one analog tape track. A standard IRIG constant bandwidth multilexer will be used to multiplex the nine sets of data. The data format will be similar to the following table.

Table 6-2 Example Data Format

CHANNEL ASSIGNMENT	IDENTIFYING FREQUENCY (Hz)	DATA NAME
1	20.8	H-H Constant Gate
2	29.2	H-H Variable Gate
3	37.5	H-V Constant Gate
4	45.8	H-V Variable Gate
5	54.2	V-V Constant Gate
6	62.5	V-V Variable Gate
7	70.8	V-H Constant Gate
8	79.2	V-H VAriable Gate
9	87.5	Calibrate Data

Possible Channel and Frequency Assignments

The data has a carrier frequency of 500 Hz and a bandwidth of 1000 cps. The frequency deviation of channel two, for example, may vary from 20.3 KHz to 21.3 KHz, where the negative doppler will range from 20.3 to 20.8 KHz and the positive doppler from 20.8 KHz to 21.3 KHz. Each of the four polarizations is recorded on one channel of a IRIG constant bandwidth multiplexer.

The horizontal-transmit/horizontal-receive fixed gate data, as shown in Table 6-1, is recorded on channel 1. The identical information which may be modified by a variable gate is recorded on channel 2. Hence, eight sets of data are available to the investigator for processing. The ninth channel contains system calibration constants needed by the computer for recorded power level. The system operating mode and gain signals are positioned in frequency from 366 to 434 Hz and 513 to 792 Hz, respectively. The transmitter power reference and the calibrate power reference signals are at 500 and 1000 Hz respectively.

The calibration constants of the 400 MHz scatterometer are determined both by the amplitude and the frequency of the signals in the calibration channel. Thus, the computer program must be modified to solve for constants.

The amplitudes of the 200 and 1000 Hz signals in the calibrate receiver must be comparéd by the computer to solve for the ratio of the transmitted to calibrate signal power. The formula for solving this ratio is P_T/P_C, where P_T is the amplitude of the 500 cps signal and the P_C is the amplitude of the 1000 cps signal.

To solve for the ratio of power of a given angle the computer must compare the amplitude of i^{th} channel to the calibrate signal using the equation P_{RC}/C_R, where P_{RC} is amplitude of the received power in the i^{th} channel and C_R is power in calibrate receiver.

The frequency of the signals within the calibrate receiver will not always be 500 and 1000 Hz, since the 400 MHz system uses an incremental frequency setting to denote the gain settings of the horizontal and vertical receivers. Thus, the 500 Hz signal may be positioned between 50 and 500 Hz and the 1000 Hz signal between 500 and 1050 Hz. Therefore, the computer program must search the frequency spectrum of 50 to 1050 Hz for the appropriate calibration signals. As the signal frequency is located, the receiver gain adjustments may be found from a table for the gain settings of the associated horizontal and vertical polarized receivers.

The 400 MHz scatterometer has two signal outputs for each polarized signal combination. For each polarization selected a complete positive and negative doppler spectrum is obtained from the constant gate channel. This data is in the form of amplitude versus frequency deviation about the carrier frequency of 500 cps. The variable gate channel has the capability of producing identical information. However, the variable gate channels may select any segment of the frequency spectrum desired by the investigator. This option gives the investigators added control over the data being recorded.

Three antenna gain tables are needed for reduction of the 400 MHz scatterometer data. The horizontally and vertically polarized antennas have a different antenna gain value requiring separate measurements for each polarized signal recorded. The vertical-transmit/horizontal-receive table is identical, however, to the horizontal-transmit/vertical-receive table. Hence, only three antenna gain tables are required for the following conditions:

1. H-H
2. H-V } Identical Tables
   V-H
3. V-V

Amplifier rolloff tables may be required at a later date.

6.5.2 Specific Equations

There are several basic equations which will play a part in the computer analysis of the 400 MHz scatterometer data. Three of the most essential equations are presented here, the remaining ones can be derived from these.

First, the σ_o equation:

$$\sigma_o(\theta) = \frac{2(4\pi)^3\ Vh^2\ L_m\ L_s\ W_s\ R(D)}{P_t\ \lambda^3\ G_o^2\ f'(\theta)\ \beta_\phi\ \delta^2}$$

where

P_t = peak transmitted power

$G_o^2F'(\theta)$ = two-way antenna gain pattern (table to be determined)

$R(D)$ = roll-off factor (table to be determined)

λ^3 = wavelength $(2.46\ \text{feet})^3$

β_ϕ = antenna two-way lateral beam width (in radians)

δ^2 = duty cycle (variable with altitude)

$2(4\pi)^3$ = constant

V = ground speed

h^2 = altitude

L_m = signal loss in cables and attenuators

L_s = switching loss

In this equation the duty ratio δ^2 will vary with altitude and operation mode. The object will be to detect the frequency which will identify the operating mode and thereby the measured duty ratio to be used.

The parameter W_s represents the corrected channel data, i.e., the data compensated for the various gains and voltages in each processing filter. Also included in W_s is the variation in calibration signal level which is dependent on the setting of a gain switch.

$$W_s = 10 \log \frac{1}{BWI} + 20 \log \frac{E_i}{E_R} + 20 \log k_p \frac{E_c}{E_T} - K$$

where

BWI = bandwidth of I^{th} filter

E_i = amplitude of received signal in the I^{th} channel

E_R = amplitude of calibrate signal

E_c = calibrate signal voltage

E_T = transmit sample voltage

k_p = normalizing constant

K = signal reference (see Tables 6-3 and 6-4)

Table 6-3 Calibrate Signal Level "K" Factor Matrix for Fixed Gate H/H and V/H Channels

OPERATING MODE	GAIN POSITION FREQUENCIES AND CORRESPONDING K FACTORS											
	POSITION 1		POSITION 2		POSITION 3		POSITION 4		POSITION 5		POSITION 6	
	518 ± 5 Hz		533 ± 5 Hz		548 ± 5 Hz		572 ± 5 Hz		587 ± 5 Hz		602 ± 5 Hz	
	H/H	V/H	H/H	V/H	H/H	V/H	H/H	V/H	H/H	V/H	H/H	V/H
Automatic 1k - 5k ft. 370 ±4 Hz	92.4	103.6	102.4	113.6	112.5	123.6	122.4	133.5	131.8	142.5	141.5	152.6
Automatic 4k - 20k ft. 382 ±4 Hz	92.4	103.5	102.4	113.5	112.4	123.3	122.2	133.4	131.6	142.8	141.4	152.5
Automatic 16k - 40k ft. 394 ±4 Hz	92.4	103.5	102.4	113.5	112.4	123.5	122.3	133.4	131.7	142.8	1414.	152.5
Manual 1k - 5k ft. 406 ±4 Hz	90.1	101.2	100.1	111.2	110.1	121.2	120.0	131.1	129.4	140.5	139.1	150.2
Manual 4k - 20k ft. 418 ±4 Hz	89.7	100.8	99.7	110.8	109.7	120.8	119.6	130.7	129.0	140.1	138.7	149.8
Manual 16k - 40k ft. 430 ±4 Hz	90.4	101.5	100.4	111.5	110.4	121.5	120.3	131.4	129.7	140.8	139.4	150.9

Table 6-4 Calibrate Signal Level "K" Factor Matrix for Fixed Gate V/V and H/V Channels

	GAIN POSITION FREQUENCIES AND CORRESPONDING K FACTORS											
	675 ± 7 Hz		697 ± 7 Hz		719 ± 7 Hz		741 ± 7 Hz		763 ± 7 Hz		785 ± 7 Hz	
OPERATING MODE	V/V	H/V	V/V	H/V	V/V	H/V	V/V	H/V	V/V	H/V	V/V	H/V
Automatic 1k - 5k ft. 370 ±4 Hz	92.2	102.7	102.7	113.8	112.5	123.6	122.0	133.0	132.0	143.0	142.2	153.3
Automatic 4k - 20k ft. 382 ±4 Hz	92.0	103.2	102.5	113.5	112.4	123.5	121.9	133.0	131.9	143.0	192.0	153.0
Automatic 16k - 40k ft. 394 ±4 Hz	92.1	103.2	102.6	113.7	112.4	113.5	121.9	133.0	131.7	143.0	142.1	153.2
Manual 1k - 5k ft. 406 ±4 Hz	89.8	100.9	100.3	111.4	110.3	121.2	119.6	130.7	129.6	140.7	139.8	150.9
Manual 4k - 20k ft. 418 ±4 KHz	89.4	100.5	99.9	111.0	109.1	120.8	119.2	130.3	129.2	140.3	139.4	158.5
Manual 16k - 40k ft. 430 ±4 Hz	90.1	100.1	100.6	110.6	110.4	120.4	119.9	129.9	129.9	139.9	140.1	150.1

Tables 6-3 and 6-4 give the information necessary for choosing the proper K factor for insertion into the W_s equation. The choice will depend on three indicators:

(1) One of 6 frequency readings which will determine the operation mode.

(2) One of 9 frequency readings which will determine the transmit/receive mode.

(3) One of 12 frequency readings which will determine the gain setting position.

For example, a frequency of 382 ±4 Hz read from the calibrate channel of the tape says the operation mode is automatic from 4k-20k feet; frequency reading 20.8 Hz say, will indicate that the transmit/receive mode is H/H fixed gate*; and finally frequency reading 553 ±5 Hz will determine the gain setting as position 2. These readings identify Table 6-3, column 3, row 2 and yield a K factor of 102.4 db. At present only the fixed gate channels are being considered. The requirements written here will also apply to variable gate channels. Except for some slight modifications which remain unresolved the programming will be identical for both fixed and variable gate data reduction.

6.5.3 Filter Center Frequency and Bandwidth Equations

The current computer program was originally designed to compute σ_o versus θ plots using an analog filter to measure the amount of receiver power at a specified frequency. Because the analog equipment cannot be readjusted in frequency for a velocity change, it was decided to adjust the angle theta (θ) in order to qualify the σ_o versus θ plots. The equation used to accomplish this is:

*The channel frequency assignments have not been definitely set at the time of writing. It will be possible to program for these settings, however, and input the values when the assignments are made.

$$\sin\theta = \frac{\lambda D}{2V}$$

where

λ = system wavelength

D = measured doppler frequency

V = velocity

θ = computed angle for plotting σ_o

As the digital filtering program was being developed it was decided to retain the analog filtering capabilities. Therefore, the technique of measuring the amount of received power at a specified frequency was utilized. The equation relating doppler frequency to an angle of incidence is:

$$f_d(\theta) = \frac{2V}{\lambda}\sin\theta$$

where

V = aircraft velocity in knots

and

$$\frac{2}{\lambda} = 1.373 \text{ Hz/knot.}$$

For a particular mission where velocity is known in knots, Table 6-5 gives the constant K versus incidence angles of interest. With this K factor, the center frequencies for the analysis filters can be computed in the following way:

$$f_c = 1.373\,V\sin\theta$$

$$K = 1.373\sin\theta$$

$$f_c = K\,V \qquad \text{(V in knots)}$$

Table 6-5 K Factor as a Function of Incidence Angles

θ	2.5	5	10	15	20	25	30	35	40	45	50	55	60
K	.06	.12	.238	.355	.469	.58	.686	.787	.882	.971	1.052	1.125	1.189

The filter bandwidth settings are computed to correspond with a square resolution cell of constant size for all incidence angles. Each cell on the ground will have fixed length and width of 2Δd (see Figure 6-2). The bandpass limits have been defined as the doppler return frequency from the points ± half the length of a side (Δd) of a resolution cell.

From the figure, a general relation for Δd can be developed in the following manner:

$$\Delta d = R \tan 1.5° \quad \text{(from H-plane)}$$

$$R = \frac{h}{\cos \theta} \quad \text{(from E-plane)}$$

Then, the resolution cell size will be 2Δd x 2Δd where

$$2\Delta d = .05236 \frac{h}{\cos \theta}$$

A series of relationships can now be developed. The center doppler frequency constant is

$$K_{f_d} = 1.373 \sin \theta \quad \text{Hz/knot}$$

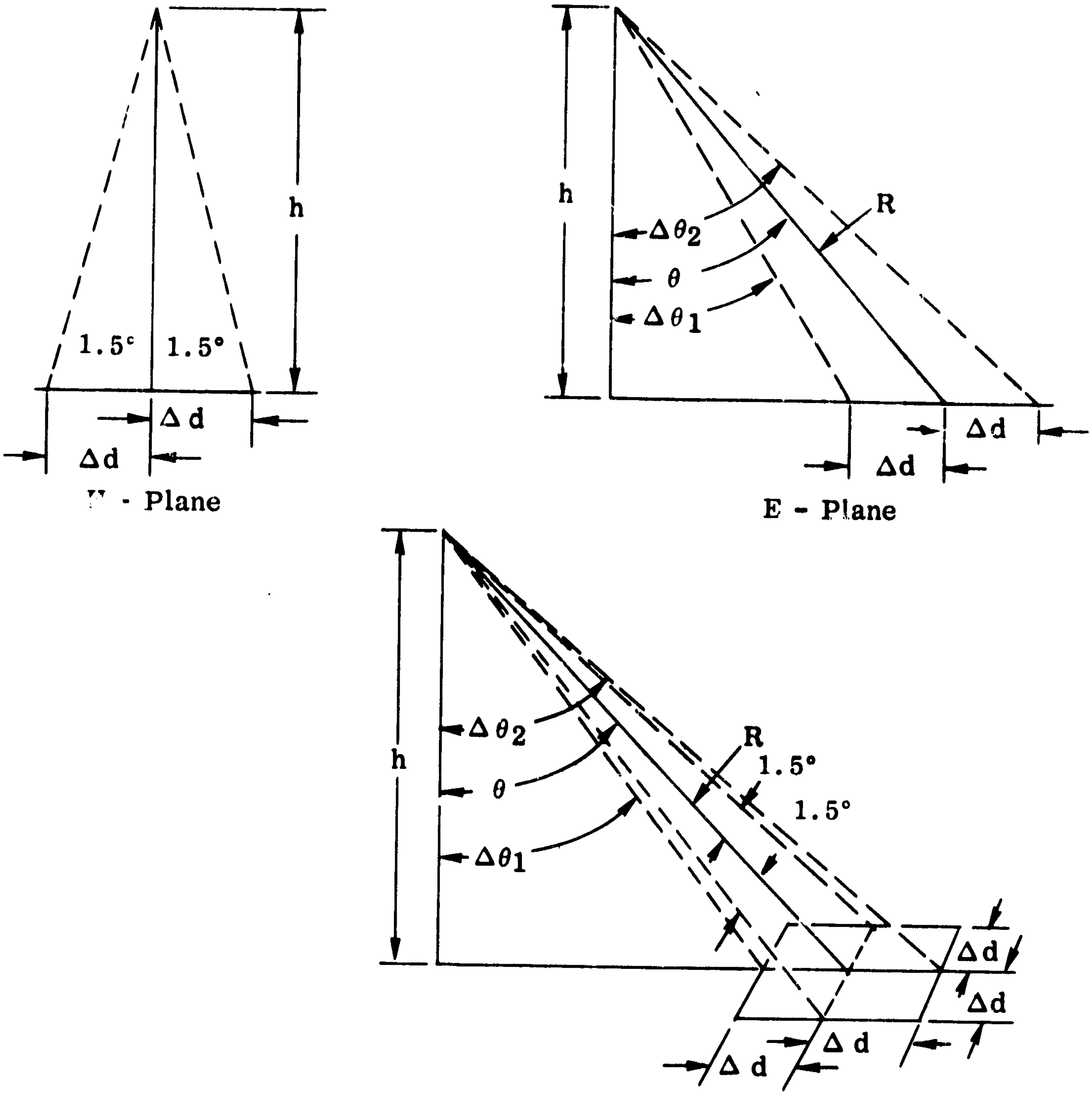

Figure 6-2 Cell Length and Width

The frequency constant for $(\theta + \Delta\theta_2)$

$$K_{f_{d+}} = 1.373 \sin(\theta + \Delta\theta_2) \quad \text{Hz/knot}$$

The frequency constant for $(\theta - \Delta\theta_1)$

$$K_{f_{d-}} = 1.373 \sin(\theta - \Delta\theta_1)$$

where

$$\theta+\Delta\theta_2 = \tan^{-1}\left(\tan\theta + \frac{\Delta d}{h}\right)$$

$$\theta-\Delta\theta_1 = \tan^{-1}\left(\tan\theta - \frac{\Delta d}{h}\right)$$

If a specific incidence angle, θ_d, is chosen for defining a standard resolution cell than $\Delta d/h$ in the above equation can be replaced by:

$$\frac{\Delta d}{h} = \tan 1.5° \sec\theta_d$$

Finally a bandwidth constant K_{BW} can be defined:

$$K_{BW} = K_{f_{d+}} - K_{f_{d-}}$$

Now to relate the center doppler frequency to the center frequency of the bandwidth the following equation were developed:

$$\text{Upper Frequency} = K_{f_d} V - \frac{K_{BW}}{2} V \quad \text{Hz}$$

$$\text{Lower Frequency} = K_{f_d} V + \frac{K_{BW}}{2} V \quad \text{Hz}$$

taking into account the 500 Hz carrier frequency the

$$\text{Actual Upper Frequency} = 500 - V\left(K_{f_d} - \frac{K_{BW}}{2}\right) \text{ Hz}$$

$$\text{Actual Lower Frequency} = 500 - V\left(K_{f_d} + \frac{K_{BW}}{2}\right) \text{ Hz}$$

The 400 MHz digital filtering program was developed using the variable doppler frequency concept to compensate for the variation in aircraft velocity. The equation for programming variable center frequencies for each angle of θ can be derived from the information previously related. The equation used in the 400 MHz program for variable center frequencies and bandwidths is:

$$f_c(\theta) = 1.373 \text{ V} \sin\theta \quad \text{Hz}$$

where

V = aircraft velocity in knots

θ = angle of incidence from nadir

This equation can be programmed to vary the center frequencies of the filters for each angle of θ as velocity of the aircraft varies.

To set the bandwidths of the filters the following equation has been developed:

ΔF = upper bandwidth setting - lower bandwidth setting

$$\Delta F = 1.373 \text{ V} \left\{\sin\left[\tan^{-1}(\tan\theta + C)\right] - \sin\left[\tan^{-1}(\tan\theta - C)\right]\right\} H_z$$

Here, ΔF is the filter bandwidth determined by a choice of incidence angle (θ). As with center frequency, bandwidth is variable with aircraft velocity (V) given in knots. The constant C is a resolution cell size factor defined as follows:

$$C = \sec \theta_d \tan \frac{BW}{2}$$

where

ϕ_d = defining angle of incidence

BW = port-starboard beadwidth at θ_d

For the present θ_d can be chosen at 30° and BW as 3° yielding:

$$C = \sec 30^\circ \tan 1.5^\circ$$

$$= .03024$$

It is felt that C should be programmed as variable so that upon receipt of accurate boresight data either θ_d and/or BW may be changed.

SECTION 7

REFERENCES

1. Bowditch, Nathaniel, American Practical Navigator, Washington, Navy Hydrographic Office, 1958, Pub. No. 9.

2. Rouse, John W., "Preliminary Mission Analysis Report NASA/MSC Mission No. 47, Site 93, Pt. Barrow, Alaska," CRES Report, Center for Research, Inc., University of Kansas, Lawrence, Kansas, October 1967.

3. Maling, George C., et al., "Digital Determination of Third-Octave and Full-Octave Spectra of Acoustical Noise," IEEE Trans Audio and Electrocoustics, Vol. AV-15, No. 2, p. 98, June 1967.

4. Cochran, W. T., et al., "What is the Fast Fourier Transform?" Proc. IEEE, Vol. 55, No. 10, October 1967.

5. Davies, H., "The Reflection of Electromagnetic Waves From a Rough Surface," Proc. IEEE, Part III, vol. 101, pp. 209-214, 1954.

6. Hayre, H. S. and R. K. Moore, "Theoretical Scattering Coefficient For Near Vertical Incidence From Contour Maps," J. Res. NBSD. Radio Propagation, Vol. 65-D, pp. 427-432, 1961.

7. Beckman, P., "Scattering by Composite Rough Surfaces," Proc. IEEE., Vol. 53, pp. 1012-1015, August, 1965.

8. Fung, A. K., "Scattering Theories and Radar Return," CRES Report 48-3, University of Kansas, May, 1965 (dissertation).

9. Moore, R. K., and W. J. Pierson, "Measuring Sea State and Estimating Surface Winds from a Polar Orbiting Satellite," University of Miami International Symposium on Remote Sensing, November 1965.

10. Janza, F. J., "The Analysis of a Pulsed Radar Acquisition System and a Comparison of Analytical Models for Describing Land and Water Radar Return Phenomena," Ph.D. thesis, The University of New Mexico, 1963. Also published as Sandia Corporation Monograph SCR-533, Sandie Corporation, Albuquerque, N. M., 1963.

11. Moore, R. K., "Resolution of Vertical Incidence Radar Return into Random and Specular Components," University of New Mexico, Albuquerque, Eng. Exp. Sta. Tech. Report EF-6, July 1967 (also Sandia Corp., Report SCR-6).